Review

Sustainable Sorbent Materials for Phosphorus Removal and Recovery from Wastewater: A Comprehensive Review and TRL-Based Evaluation

Ruta Ozola-Davidane [1,*], Kamila Gruskevica [2,*], Oskars Purmalis [3], Solvita Kostjukova [4,5], Julija Karasa [4], Ivar Zekker [6], Sandija Ozolina-Grinevica [1], Andrejs Krauklis [7]

[1] Institute of Landscape Architecture and Environmental Engineering, Faculty of Forest and Environmental Sciences, Latvia University of Life Sciences and Technologies, LV-3001 Jelgava, Latvia; sandija.ozolina-grinevica@lbtu.lv (SO-G)

[2] Water Systems and Biotechnology Institute, Faculty of Natural Sciences and Technology, Riga Technical University, LV-1048 Riga, Latvia

[3] Department of Environmental Science, Faculty of Science and Technology, University of Latvia, LV-1004 Riga, Latvia; oskars.purmalis@lu.lv (OP)

[4] The Faculty of Medicine and Life Sciences, University of Latvia, LV-1004 Riga, Latvia; solvita.kostjukova@lu.lv (SK); julija.karasa@lu.lv (JK)

[5] The Faculty of Economics and Social Sciences, University of Latvia, LV-1050 Riga, Latvia

[6] Chair of Colloidal and Environmental Chemistry, Institute of Chemistry, Faculty of Science and Technology, University of Tartu, 50411 Tartu, Estonia; ivar.zekker@ut.ee (IZ)

[7] MEI Group, Institute of Civil Engineering and Woodworking, Faculty of Forest and Environmental Sciences, Latvia University of Life Sciences and Technologies, Jelgava LV-3001, Latvia; akraukli@lbtu.lv (AK)

* Correspondence: Ruta Ozola-Davidane, Email: ruta.ozola-davidane@lbtu.lv; Kamila Gruskevica, Email: kamila.gruskevica@rtu.lv.

ABSTRACT

The removal and recovery of phosphorus (P) from wastewater is critical for preventing eutrophication and achieving sustainable nutrient management. This review critically evaluates sustainable sorbent materials for P removal and recovery, focusing on mineral-based, bio-based, and recycled sorbents derived from industrial by-products. It compares their P removal efficiencies, adsorption mechanisms, environmental impact, and regeneration potential. A structured application of the Technology Readiness Level (TRL) framework is used to evaluate the maturity, scale-up feasibility, and real-world implementation potential of the reviewed P sorbents. The TRL-based assessment complements performance comparisons by explicitly considering cost-effectiveness, regulatory and policy alignment, and compatibility with existing wastewater treatment infrastructure. Sustainability aspects are addressed through lifecycle-relevant criteria, including regenerability

Open Access

Received: 11 Feb 2026
Accepted: 22 Apr 2026
Published: 07 May 2026

and reuse potential and valorisation pathways for spent sorbents (e.g., reuse as soil amendments or slow-release fertilisers). The review concludes by identifying key evidence gaps (notably long-term validation in real wastewater and robust regeneration/P-recycling routes) and outlining research priorities to accelerate the development of efficient, scalable, and environmentally viable solutions for phosphorus recovery in wastewater treatment.

KEYWORDS: phosphorus recovery; sustainable sorbents; adsorption; wastewater treatment; technology readiness level

ABBREVIATIONS

WWTP, wastewater treatment plant; TRL, Technology Readiness Level; PRISMA, Preferred Reporting Items for Systematic Reviews and Meta-Analyses; NASA, National Aeronautics and Space Administration; LDH, layered double hydroxides; LCA, Life Cycle Assessment; REE, Rare Earth Element; EPS, Extracellular Polymeric Substances; PVDF, Polyvinylidene Fluoride; GHG, Greenhouse Gas; BET, Brunauer–Emmett–Teller; XRD, X-ray diffraction; ACTW, amine cross-linking of spent tea leaves

INTRODUCTION

Urbanisation, industrialisation, and intensive agriculture are causing an increase in phosphorus (P) levels, impairing water quality and sustainability. One of the most important environmental challenges associated with excess P in aquatic systems is eutrophication. Elevated P concentrations stimulate harmful algal blooms and oxygen depletion, significantly diminishing water quality and biodiversity [1]. Eutrophication poses a substantial threat to ecological stability, fisheries, and recreational water use, making effective P removal a fundamental goal for wastewater treatment plants (WWTPs). In response, regulatory agencies worldwide have tightened discharge standards, often requiring treated effluents to contain < 1 mg P/L [2]. This escalation in regulatory stringency has driven the development and implementation of more effective and reliable P-removal technologies, as many WWTPs currently rely on chemical precipitation or enhanced biological P removal to comply with environmental regulations [3].

The need for improved P management in wastewater is also rooted in sustainability and resource security. P is a limited, non-renewable resource predominantly obtained through phosphorite rock mining. Concerns over the long-term availability and geopolitical distribution of P reserves have intensified interest in P recovery from wastewater streams [4]. By extracting and reusing P as a fertiliser, WWTPs can shift from a linear disposal model to a more circular system, thereby promoting agricultural resilience and reducing reliance on raw P sources.

Conventional methods for P removal achieve significant P reduction in effluents, but generate large volumes of sludge and secondary pollution due to residual metals in the treated effluent [5]. Biological methods can reduce chemical use and facilitate resource recovery, although they remain complex, sensitive to operational conditions, and still produce sludge [6]. These limitations highlight the need for alternative or complementary approaches that balance high removal efficiency, cost-effectiveness, environmental compatibility, and operational simplicity.

In this context, the development and application of sorbent-based technologies have gained attention as a promising strategy for P removal and recovery. Recent studies demonstrate that natural and modified sorbents can achieve efficient nutrient removal, providing enhanced selectivity, reduced chemical consumption, and the potential for their regeneration and reuse [7–9]. Certain sorbents can simultaneously target multiple contaminants, streamline treatment processes, and reduce overall system complexity [10,11].

A sustainable sorbent can be defined as a material that is designed and produced in an environmentally-friendly and resource-efficient manner, while also exhibiting desirable properties for effective pollutant removal and potential for reuse or regeneration. These attributes align with efforts to minimise environmental impacts, lower treatment costs, and ensure long-term ecological stability [12–18]. In practical terms, this implies that sustainable sorbents should combine low energy and chemical requirements during production, the use of abundant or waste-derived materials, cost-effectiveness, high removal performance, and the ability to be regenerated, reused, or safely valorized after use.

This review provides a rigorous and up-to-date evaluation of sustainable sorbent materials and technologies for P removal and recovery from wastewater, synthesising findings from research articles published within the last ten years. Focusing on mineral-based, bio-based, and recycled materials derived from industrial by-products, the paper critically examines their removal efficiencies, sorption mechanisms, environmental impacts, and potential for full-scale implementation, while also addressing the regeneration and recycling of spent sorbents to assess their long-term sustainability. As part of this analysis, the TRL framework is applied to assess the maturity and real-world feasibility of these technologies. By comparing innovative and conventional P removal methods, this review aims to inform researchers, engineers, and policymakers on more sustainable, efficient, and cost-effective strategies for P management in wastewater treatment.

METHODOLOGY

The systematic literature review was conducted in accordance with the PRISMA (Preferred Reporting Items for Systematic Reviews and Meta-Analyses) guidelines [19] to ensure methodological transparency, traceability, and reproducibility. During the identification phase, a

comprehensive search was performed across electronic databases, including Scopus, Clarivate Web of Science (Core Collection), ScienceDirect. Boolean operators (*AND, OR*) were used to construct the search strategy, integrating the following keywords and combinations*: "phosphorus removal", "phosphate adsorption", "sorbent", "sustainable sorbents", "biochar phosphorus", "mineral-based sorbents", "industrial by-products", "wastewater"*. Only peer-reviewed research articles were used. The search was restricted to publications from the past ten years, although earlier foundational studies were included where scientifically justified.

Following the removal of duplicate records, an eligibility assessment through full-text review was made, based on predefined inclusion criteria: (i) quantitative or qualitative evaluation of P removal efficiency; (ii) characterisation of sorption mechanisms; (iii) relevance to sustainable, mineral-based, bio-based, or industrial-by-product sorbents; and (iv) applicability to wastewater treatment contexts. The final set of eligible articles was incorporated into the qualitative synthesis and subsequently categorised by sorbent type and technology maturity to support comparative evaluation. Some references may be repeated across Tables 1–3 because information on different materials was obtained from the same article. The PRISMA flow diagram, detailing the study selection process and exclusion rationale, is provided in Figure S1.

To move beyond performance reporting and to address feasibility for implementation, this review applies the TRL framework. TRLs provide a common language to track progress from early research to operational deployment and are widely used across domains where scale-up, compliance, and system integration are decisive barriers (e.g., environmental engineering applications). TRL is a standardised nine-level scale originally developed by NASA and is widely used in fields such as defence [20], pharmaceuticals [21], and environmental engineering [22] to assess technology maturity from basic research to full commercialisation. The TRL scale categorises technological development into 9 distinct levels, from initial concept (TRL 1) through to actual system proven in an operational environment (TRL 9) [21,23].

TRL values were assigned based on the highest demonstrated stage reported in the literature only when supported by explicit evidence of scale and environment, not on theoretical potential. For each technology/material, we screened for: (i) test environment (synthetic vs real wastewater/effluent); (ii) system configuration (batch vs column/continuous); (iii) degree of process integration; and (iv) validation context (lab vs. pilot vs operational setting).

The TRL classification approach applied in this study is illustrated in Figure 1. The following criteria were used for TRL assignment:

- TRL 1–2: Novel materials demonstrated only in theoretical models or fundamental lab-scale studies, without application to real wastewater.
- TRL 3–4: Bench-scale proof-of-concept (synthetic/spiked/simplified matrices), limited system integration.
- TRL 5–6: Pilot-scale systems operated using real wastewater under controlled conditions; partial integration into existing treatment processes.
- TRL 7–8: Demonstration in operational WWTP; full process integration; supported by economic and regulatory feasibility studies.
- TRL 9: Technology commercially deployed and standardised; included in national/regional regulations or accepted by WWTP operators.

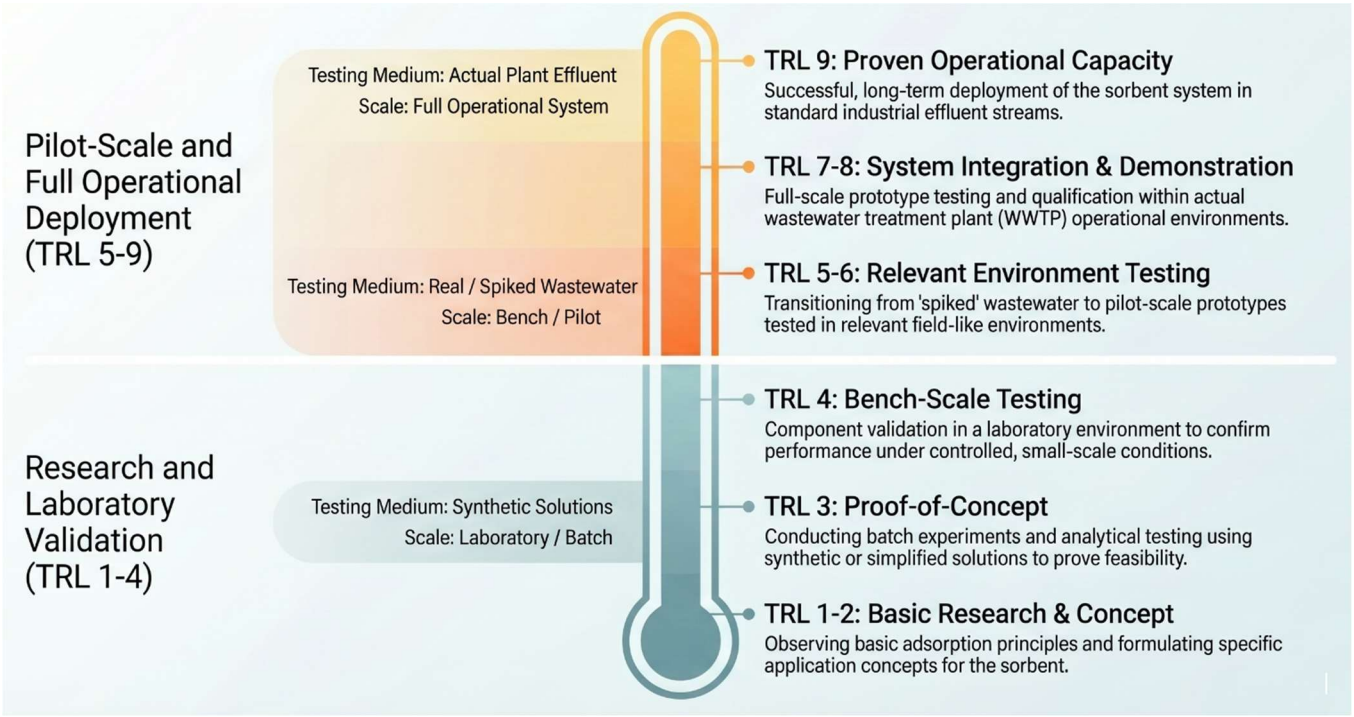

Figure 1. Adapted TRL framework for P sorbent technologies, illustrating the progression from laboratory (TRL 1–4) to pilot (TRL 5–6) and full-scale (TRL 7–9) implementation in wastewater treatment systems (image generated with ChatGPT).

Conservative rule for ambiguous cases. When literature evidence was insufficient to confirm pilot/field integration (e.g., missing matrix definition or unclear operational context), the TRL assignment was not upgraded, and the technology remained at the lower TRL consistent with available evidence. This addresses reviewer concerns about over-interpreting laboratory results and mixing non-comparable studies.

The TRL definitions applied in this review follow the Horizon Europe Work Programme General Annexes [24], where TRL levels are specified when required by call/topic conditions, and this approach is consistent with recent wastewater phosphorus recovery reviews that report technology maturity using TRL [25].

MINERAL-BASED SORBENTS FOR P REMOVAL FROM WASTEWATER

Mineral-based sorbents, including lanthanum, zirconium, and iron compounds, as well as zeolites, clays, and layered double hydroxides (LDHs), have been extensively studied for P removal due to their strong binding affinity, stability, and potential for regeneration. These materials exhibit diverse removal capacities, operating mechanisms, and pH applicability.

Lanthanum-Based Sorbents

Lanthanum (La)-based materials have shown high affinity for P due to strong ligand exchange and inner-sphere complexation. Among these, La–zeolite hybrid sorbents such as La-ZFA achieved >95% P removal across a wide pH range (pH 2.5–10.5), with an adsorption capacity of 23.5 mg P/g. P uptake was driven by ligand exchange and $LaPO_4$ formation, while 3M NaOH at 250 °C enabled regeneration of both La-ZFA and sorbed P [26]. Similarly, La-impregnated zeolite (NLZ) improved P uptake to 2.9 mg P/g (vs. 0.07 mg P/g for raw zeolite), primarily through formation of $(LaO)(OH)PO_2$, with minor pH dependence below pH 7 [27].

A cost-effective HPAL-LaOH sorbent, prepared by loading $La(OH)_3$ onto calcined nano-porous palygorskite via hydrothermal synthesis, achieved a high P adsorption capacity (35.77 mg/g), over 13 times higher than raw palygorskite and exceeding that of commercial $La(OH)_3$ (22.72 mg/g). HPAL-LaOH achieved near-complete P removal across pH 3–11, showed minimal impact from competing anions, and showed excellent stability, sedimentation behaviour, and reusability with negligible La leaching [28].

Similarly, in line with circular economy principles, Kasprzyk and Gajewska [29] tested two La-based natural sorbents, i.e., M1 (Rockfos®), a waste from thermally treated carbonate-siliceous rock, and M2, La-modified bentonite. They achieved P sorption capacities of 45.6 mg P/g (M1) and 5.6 mg P/g (M2) in synthetic wastewater.

Another bio-based alternative, a La-incorporated chitosan membrane (La@CS) prepared via casting, showed up to 25.0 mg P/g adsorption capacity. The main sorption mechanisms were electrostatic attraction and ion exchange between the membrane and PO_4^{3-} [30].

Further advancement was made with MALZ, a La-incorporated nanostructured ternary (hydr)oxide sorbent with evenly distributed Mg, Al, and La on a zeolite [31]. MALZ showed rapid and efficient P removal across pH 4–10, reaching 80.8 mg P/g at pH 6.6 (12.5 wt% La). Coexisting anions (Cl^-, SO_4^{2-}, NO_3^-) had no significant effect on adsorption. MALZ maintained 75.8% of its capacity after four regeneration cycles using 0.5 M NaOH. Main sorption mechanisms included electrostatic attraction, ligand exchange, and inner-sphere complexation ($LaPO_4{\cdot}xH_2O$), with Mg and Al enhancing La dispersion and surface charge.

Wei et al. (2020) [32] developed a La-Zr-Zn ternary oxide with 52.08 m^2/g surface area, achieving >97% P removal efficiency at 0.2 g/L and pH 5–9. Adsorption followed pseudo-second-order kinetics and Langmuir model, with a capacity of 23.36 mg P/g at pH 6.8. La-modified natural (LZ) and magnetic zeolites (LMZ) reached 122.7 and 109.17 mg P/g, respectively, via inner-sphere complexation and electrostatic attraction. Additionally, LZ and LMZ acted as sediment passivators by transforming unstable iron-bound and organoclastic P into stable aluminium- and calcium-bound forms, thereby reducing its bioavailability. LMZ also demonstrated magnetic recyclability and superior capacity to adsorb active P [33].

High CO_2 burden is associated with La-based adsorbent preparation, as rare earth element (REE) mining, extraction, and purification involve energy-intensive, multi-stage processes requiring strong acids and bases. Life Cycle Assessment (LCA) studies report substantial energy demand (e.g., ~177 MJ/kg for La_2O_3) and greenhouse gas emissions ranging from ~9 to >60 kg CO_2-eq per kg of rare earth oxides, depending on the production route, highlighting a significant environmental footprint per unit of final sorbent [34]. Longer lifetime of ZnFeZr adsorbent in P desorption and adsorbent regeneration has been demonstrated with over 60 cycles using NaOH solution for the ZnFeZr adsorbent immobilised on Fe_3O_4/SiO_2 [35]. The high cost of La salts further limits scalability relative to Fe- or Ca-based sorbents. Improving P adsorption efficiency is often achieved by immobilising La onto a wide array of stable, porous, and low-cost carriers. These diverse substrates span inorganic materials (magnetic Fe_3O_4, clay minerals, mesoporous silica), synthetic polymers (hydrogel, ion exchange resin), and carbonaceous derivatives (graphene, chitosan, agricultural/forestry wastes, and biochars). The spent La-phosphate product is a highly valuable, recoverable as P and La source, offering a strong economic incentive that offsets the high initial material cost [36].

Zirconium-Based Sorbents

Zirconium (Zr)-based sorbents have demonstrated good affinity for P due to strong ligand exchange, electrostatic interaction, and inner-sphere complexation mechanisms. Several composite materials have been developed to enhance their capacity, stability, and reusability.

A Zr^{4+}-loaded okara sorbent (ZLO), prepared by impregnating soya bean waste with Zr^{4+} solution, has shown a dynamic adsorption capacity of 5.36 mg P/g in fixed-bed columns, with regeneration achieved using 0.2 M NaOH and 0.1 M HCl [37].

Novel zirconium-pillared montmorillonites (Zr-Mt and Zr/Al-Mt), prepared by introducing Zr^{4+} and Zr^{4+}/Al^{3+} into montmorillonite clay (Mt), has shown enhanced surface area and a maximum sorption capacity of 17.2 mg P/g [38]. Adsorption followed pseudo-second-order and Langmuir models, was spontaneous and endothermic, and most effective at pH 3. Competitive ions had minor effects, except CO_3^{2-}, leading to decreased

adsorption efficiency. Zr leaching was negligible over pH 3–9, and the sorbents retained adsorption efficiency after three cycles.

Amorphous Zr hydroxide, tested both in batch and submerged membrane–filtration hybrid reactors (MFAH), showed Langmuir capacities from 18.5 to 54.6 mg P/g. Although performance declined after 5 h in MFAH, periodic Zr hydroxide addition restored removal efficiency for up to 3 days [39].

Zr/Fe oxide-loaded activated carbon nanofibres (ACF-ZrFe) achieved 26.3 mg P/g capacity at pH 4.0, with removal governed by ligand exchange and electrostatic attraction. Co-existing ions ($F^- > NO_3^- > Cl^- > SO_4^{2-}$) in solution showed varied effects on P adsorption, which was affected by ligand exchange and electrostatic interactions as dominant mechanisms [40].

Chitosan–bentonite composites modified with Zr^{4+}, Fe^{3+}, and Ca^{2+} (Zr@CSBent, Fe@CSBent, Ca@CSBent) exhibited capacities of 13.33, 7.23, and 4.39 mg P/g, respectively. The sorption mechanisms varied among composites, involving ion exchange, electrostatic interaction, and inner-sphere complexation [41].

A Zn/Al/Zr-layered double hydroxide (ZARH) composite with hydrothermal carbon loading was synthesised via co-precipitation to enhance P removal from wastewater [42]. Microstructural analysis revealed that the ZARH-3 composite had a high specific surface area and abundant active sites. Under simulated conditions, it removed 99% of P (25 mg P/L) within two hours, achieving a maximum adsorption capacity of 26.64 mg P/g at pH 5. Adsorption followed Langmuir and Temkin isotherms ($R^2 > 0.99$), driven by ion exchange, electrostatic attraction, and ligand exchange mechanisms.

Zr salts (e.g., $ZrOCl_2$, $ZrCl_4$) typically are not waste-derived materials but are synthesised from Zr sand ($ZrSiO_4$) via energy-intensive thermal and acid/chlorination processes, resulting in a substantial LCA footprint [43,44].

Iron-Based Sorbents

Various iron-based sorbents have been investigated for P removal from wastewater, including zero-valent iron/sand materials [45], Cu-chitosan/Fe_3O_4 nanocomposites [46], Ce-incorporated zinc ferrites [47], iron doped clays [48], TiO_2/Fe_3O_4 composites [49] and sodium alginate based (SA)-Fe(III) extracellular polymeric substances (EPS)-like hydrogels [50].

The highest P adsorption result (134.33 mg P/g) was achieved using (SA)-Fe^{3+} (EPS)-like hydrogel, a cheaper alternative to natural EPS based hydrogels. Surface adsorption was noted at initial P concentrations of 0–35 mg/L, shifting to internal diffusion control at higher concentrations [50].

All iron-based sorbents described here showed best performance in neutral pH range. In initial stages several studies demonstrated chemical P adsorption driven by electrostatic attraction and ligand exchange

[45,46,50]. After equilibrium conditions were reached, adsorption shifted to P diffusion to internal layers [48,50].

P-saturated HA@SA-Fe^{3+} hydrogels demonstrated potential as sustainable-release P fertilisers [50], while doped clay-based sorbents were deemed for one-time applications [48], other materials may be reused up to five cycles using alkalis for P desorption [47,49]. Magnetite mineral microparticles (Mag-MM) also demonstrated high reusability. In real secondary wastewater effluent, they achieved up to 0.83 mg P/g while consistently reducing effluent P levels below 0.1 mg/L over 30 reuse cycles. P recovery was facilitated via $CaCl_2$-induced precipitation, and alkaline regenerants such as NaOH, $KHCO_3$, or Na_2CO_3 showed better desorption efficiency than sodium acetate [51].

Utilising Fe-rich industrial wastes (e.g., steel slag, Fe-rich sludge) avoids landfilling and land-use impact, providing a direct LCA credit and near-zero adsorbent producing costs. Some Fe-composites (like Fe-biochar) require pyrolysis/calcination (typically 300–700 °C). The energy input for this step contributes the most CO_2 to the final material. However, the energy input is often lower than for Ca-based materials since the goal is stabilisation, not calcination. Acid mine drainage oxides, steel slag, Fe-rich sludges have low processing costs. Fe-modified biochar, Fe oxy-hydroxides (goethite, ferrihydrite), Fe-doped clays have relatively medium costs while the cost of goethite-modified biochar (BC-Gt) (80–130 $/t) is 10%–20% higher as compared to BC (80–90 $/t) and Gt (70–120 $/t) [52].

Zeolite-, Clay-, and Layered Double Hydroxide (LDH)-Based Composites

Zeolite-based materials exhibit promising P removal efficiencies due to their porous structure and ion exchange capacity. A TiO_2/zeolite (TZ) composite achieved ~100% P removal at low concentrations, with 12.3 mg P/g adsorption capacity, via electrostatic attraction and surface hydroxyl substitution [53]. Similarly, the hybrid sorbent ZIF-8 (a zeolitic imidazolate framework) demonstrated a monolayer chemisorption mechanism and 12.47 mg P/g sorption capacity, though performance decreased in the presence of carbonate ions [54]. Compared to ZIF-8, ZIF-67 showed significant reusability maintaining over 90% efficiency after six adsorption–desorption cycles [55]. These results suggest that zeolite-based materials not only offer effective adsorption but also have high regeneration potential.

Modified natural zeolites such as Ca $(OH)_2$-treated zeolite (CaT-Z) demonstrated strong inner-sphere complexation (ligand exchange) and higher binding efficiency in human urine than raw zeolites. CaT-Z achieved up to 11.11 mg P/g and enabled partial P recovery via sequential desorption [56]. MgO/iron-oxide modified NaY zeolite (MNZ) further enhanced simultaneous ammonium and P removal through struvite precipitation, reaching 105.95 mg P/g and suggesting potential application in slow-release fertiliser [57].

Calcined layered double hydroxide (LDH) nano-composites exhibited P adsorption capacities exceeding 100 mg/g, primarily through ion exchange, while regeneration with NaOH induced a dissolution–reprecipitation process that facilitated LDH recrystallization. Ammonia-based regeneration facilitated struvite crystallization and produced slow-release fertilisers with enhanced P bioavailability [58]. LDH-modified biochars have also emerged as promising sorbents. Yang et al. (2019) [59] prepared Zn/Al-, Mg/Al-, and Ni/Fe-based LDH–biochar composites via co-pyrolysis, achieving adsorption capacities up to 152.1 mg P/g through interlayer anion exchange and surface complexation. P removal efficiency was affected by pH and the presence of other anions in the solution. Zhang et al. (2022) [60] further demonstrated efficient P removal from real secondary wastewater using similar LDH–biochar composites (Zn–Al, Mg–Al, and Mg–Fe LDH/BC), with capacities between 35.2 and 55.8 mg P/g. When applied as fertilisers, Mg– and Fe–based LDH/BCs promoted crop growth more effectively than Zn–based materials, linking P bioavailability and physiological impact on crops.

Finally, a clay–polymer composite membrane incorporating polyvinylidene fluoride (PVDF) demonstrated potential as an emerging clay–polymer sorbent, achieving P uptake of 0.75 mg/g within six hours due to porous and heterogeneous structure [61]. Although current performance is limited, further optimisation could enhance its applicability.

Natural zeolites and clays (e.g., bentonite, kaolin) as well as calcium-rich natural sorbents such as marl, travertine, and opoka, are geologically abundant and require only mining and minimal processing (crushing, washing). This contributes to near-zero costs and minimal CO_2 footprint [62,63]. These calcium-based materials have also demonstrated high phosphorus removal efficiencies (often >90%), which can further increase after thermal modification [63]. LDHs and many modified clays exhibit excellent regenerability (often >90% capacity after multiple cycles) using dilute NaOH, which is key to offsetting the initial synthesis cost and maximizing economic life cycle.

All mineral-based sorbents are classified at TRL 3–4, corresponding to the bench-scale proof-of-concept stage. These materials, including La-modified zeolites, Zr-based composites, Fe-based hydrogels, and LDH-derived sorbents, have demonstrated high P removal efficiencies, often exceeding 90%, and substantial adsorption capacities under controlled laboratory conditions. However, the majority of studies have been conducted using synthetic solutions or spiked matrices, with limited validation in real or long-term wastewater treatment scenarios. As a result, despite promising performance, further advancement beyond TRL 4 is limited by the lack of long-term testing, standardised evaluation methods, and validation in real wastewater treatment systems.

A comparative overview of mineral-based sorbents, their removal performance, and operating conditions is presented in Table 1.

Table 1. Adsorption of P by metal-based and mineral sorbents.

Material	Initial concentration, mg/L	Removal efficiency, %	Adsorption capacity, mg/g	Sorption mechanism	Phosphorus medium	TRL level	Ref.
Lanthanum-based sorbents							
La-ZFA	10–500 mg/L	>95%	23.48 mg P/g*	La-P precipitation; Ligand exchange	Synthetic solution	3–4	[26]
Commercial pure $La(OH)_3$	5–1000 mg/L	N/A	22.72 mg P/g*	Surface adsorption (heterogeneous sites)	Synthetic solution	3–4	[28]
HPAL-LaOH	5–1000 mg/L	>90% (in presence of competing ions)	35.77 mg P/g*	Inner-sphere complexation via ligand-exchange	Synthetic solution	3–4	[28]
La-modified bentonite (M2)	5–100 mg/L	99%	1.82 mg P/g*	Surface adsorption (heterogeneous monolayer)	Synthetic solution	3–4	[29]
La-incorporated chitosan membrane (La@CS)	50–150 mg/L	>99%	25.0 mg P/g*	Electrostatic attraction; Ion exchange	Synthetic (P with nitrate)	3–4	[30]
La-incorporated nanostructured ternary (hydr)oxide MALZ (12.5 wt% La)	1–5 mg/L	N/A	80.8 mg P/g	Electrostatic attraction; Ligand exchange; Inner-sphere complexation	Synthetic solution	3–4	[31]
La–Zr–Zn ternary oxide (La–Zr–Zn)	0.5–2 mg/L	>97%	23.36 mg P/g*	Surface adsorption (monolayer)	Synthetic solution	3–4	[32]
La-modified natural zeolite (LZ)	10–150 mg/L	53% after 1 h	109.17 mg P/g	Inner-sphere complexation; electrostatic attraction	Synthetic solution	3–4	[33]
La-modified magnetic zeolite (LMZ)	10–150 mg/L	55% after 4 h	109.17 mg P/g	Inner-sphere complexation; electrostatic attraction	Synthetic solution	3–4	[33]
Zirconium-based sorbents							
Zr(IV)-loaded okara (ZLO)	5.6 mg/L	85.44%	16.43 mg P/g	Zr-induced inner-sphere binding	Synthetic and real municipal wastewater	3–4	[37]
Zr/Al pillared montmorillonite (Zr/Al-Mt)	20–50 mg/L	N/A	17.2 mg P/g	Surface adsorption (monolayer)	Synthetic solution	3–4	[38]
Amorphous Zr hydroxide	10 mg P/L	>90% after 1 h	18.50 mg P/g	Inner-sphere complexation	Synthetic and synthetic wastewater	3–4	[39]
ACF-ZrFe	5 – 60 mg/L	N/A	26.3 mg P/g	Ligand exchange; Electrostatic attraction; Surface adsorption (monolayer)	Synthetic solution	3–4	[40]
Zr@CSBent Chitosan-supported bentonite biocomposite	100 mg/L	N/A	13.33 mg P/g*	Ion-exchange; Electrostatic attraction; Inner-sphere complexation	Synthetic solution	3–4	[41]
Iron-based sorbents							
Fe@CSBent	100 mg/L	N/A	7.23 mg P/g*	Ion-exchange; electrostatic attraction; Inner-sphere complexation	Synthetic solution	3–4	[41]
ZVI/sand	20 mg/L	22-34%	132 mg P/g Fe	Surface adsorption on Fe oxides	Synthetic solution	3–4	[45]
Cu–chitosan/Fe_3O_4 nanocomposite	26.2 mg/L* (120 mg P_2O_5/L)	N/A	19.21 mg P/g*	Surface adsorption (heterogeneous monolayer)	Synthetic	3–4	[46]

Ce-incorporated zinc ferrite ($ZnCe_xFe_2{-}xO_4$, x=0.48)	2–150 mg/L	N/A	13.6 mg P/g*	Ligand exchange (Fe/Ce sites)	Synthetic solution	3–4	[47]
TiO_2/Fe_3O_4 composite	10–200 mg/L	>85% after five recycling cycles	21.10 mg P/g*	Electrostatic attraction and Ligand exchange	Synthetic solution	3–4	[49]
SA-Fe^3 hydrogel	0–35 mg/L	<70.19%	134.33 mg P/g	Surface adsorption (diffusion-limited); Ligand exchange; Ion exchange	Synthetic solution	3–4	[50]
HA@SA-Fe^3 hydrogel	0–35 mg/L	<90.19%	56.00 mg P/g	Surface adsorption (diffusion-limited); Ligand exchange; Ion exchange	Synthetic solution	3–4	[50]
Magnetite mineral microparticles (Mag-MM)	1–8 mg/L	N/A	0.52–0.83 mg P/g	Physi- and chemisorption	Synthetic and real secondary wastewater	3–4	[51]
Layered Double Hydroxide (LDH) composites							
ZARH-3 composite	5 mg/L	99%	26.64 mg P/g	Ion exchange; Electrostatic attraction; Ligand exchange	Synthetic wastewater	3–4	[42]
Calcined LDH nano-composites	10–100 mg/L	N/A	100.7 mg P/g	Ion exchange; Recrystallization Surface adsorption (heterogeneous sites)	Synthetic solution	3–4	[58]
B-Zn/Al-LDH composite	10–200 mg/L	92.90%	152.1 mg P/g (B-Mg/Al-LDH-1)	Interlayer anion exchange; Surface complexation	Synthetic solution	3–4	[59]
LDH biochar composites (LDH/BCs), including Zn-Al-LDH/BC, Mg-Al-LDH/BC, and Mg-Fe-LDH/BC	5–80 mg/L	87% (initial 25 mg P/L)	35.19–55.76 mg P/g	-	Synthetic and spiked secondary wastewater	3–4	[60]
Zeolite based sorbents							
NaOH-activated and La-impregnated zeolite (NLZ)	5 mg/L	N/A	2.92 mg P/g*	La–P precipitation; Surface adsorption (heterogeneous monolayer)	Synthetic solution	3–4	[26]
TiO_2/Zeolite (TZ)	10–1000 mg/L	~100%	12.26 mg P/g*	Electrostatic attraction	Synthetic solution	3–4	[53]
Cubic zeolitic imidazolate framework-8 (ZIF-8)	10–1000 mg/L	<84.0%	12.47 mg P/g*	Chemisorption mechanism; Surface adsorption (monolayer)	Synthetic solution	3–4	[54]
$Ca(OH)_2$-treated zeolite (CaT-Z)	670.9 ± 7.6 mg/L	55.1–84.9%	11.11 mg P/g	Inner- and outer-sphere complexation	Fresh urine	3–4	[56]
MgO/iron oxide-modified NaY zeolite (MNZ)	400 mg/L	N/A	105.95 mg P/g*	Struvite precipitation; Electrostatic attraction; Ion exchange	Synthetic solution	3–4	[57]
Clay based sorbents							
M1 (Rockfos®)	5–100 mg/L	99%	14.87 mg P/g*	Surface adsorption (heterogeneous monolayer)	Synthetic solution	3–4	[29]
Ca@CSBent	100 mg/L	N/A	4.39 mg P/g*	Ion-exchange; Electrostatic attraction; Inner-sphere complexation	Synthetic solution	3–4	[41]
Raw clay C1 and C2	10–2000 mg/L	N/A	6.90 mg P/g*	Intraparticle diffusion; Surface adsorption (monolayer)	Synthetic solution	3–4	[48]
Fe-doped clay C1-Fe and C2-Fe	10–2000 mg/L	N/A	12.40 mg P/g*	Surface complexation;	Synthetic solution	3–4	[48]
Clay-PVDF	0.5–10.0 mg/L	50%	0.75 mg P/g	Surface adsorption (monolayer)	Synthetic solution	3–4	[61]

* Convert to P by multiplying 0.3261.

BIO-BASED MATERIALS FOR P REMOVAL FROM WASTEWATER

Bio-based sorbents, derived from agricultural residues, shells, and other biological wastes, have gained attention for phosphate removal due to their low cost, renewability, and reuse potential. For this review, materials are grouped as biochars, modified agricultural wastes, natural and calcined shells, and calcium-doped sorbents. Though both biochar production and calcination involve heat treatment, their conditions differ: biochars are produced at 300–800 °C under limited oxygen, while calcination occurs in oxygen-rich environments at 800–1000 °C. Biochars, rich in carbon and oxygen, are commonly reused as fertilisers or soil amendments, especially when enriched with phosphorus. In contrast, calcined products are better suited for industrial applications due to their higher reactivity and precipitation potential.

Biochars

Various biological waste materials may be utilised for production of bio-charcoal or shortened biochars including orange tree trunks [64], tea tree twigs [64], chemically modified tea waste [65], corn straw [66], soya bean stover [67], crawfish [68], pomegranate peel [69], litchi seeds [70], eggshells [71], oyster shell wastes [72], rice straw [73], palm fibres [74], sawdust [75], tobacco straw [76], walnut and almond wooden shell waste [77], bagasse [78] etc. Biochars may be used as fertilisers [66,79,80], which also decrease greenhouse gas (GHG) emissions, and immobilise heavy metals and organic contaminants [80,81].

Biochars are typically produced by pyrolysis of biomass in oxygen-limited or anoxic conditions at 300–800 °C, resulting in carbon-rich materials [78,79]. However, natural or untreated biochars have limited capacity to adsorb anionic species such as P [70,73,75]. Therefore, chemical or thermal modifications are essential to enhance P affinity. These modifications improve surface area, introduce active sites, and facilitate mechanisms such as ion exchange and ligand exchange [82]. Pretreatment often involves impregnation with metal salts like $FeSO_4$, $MgCl_2$, or $AlCl_3$ [64,66,83], with pyrolysis enhancing the structure and porosity of the final product. The P adsorption capacity increases in the following sequence: raw biowaste > biochar > modified biochar.

Surface area plays a critical role in adsorption efficiency and may increase by up to 200 times after modification [84–86]. However, surface area can also decrease at excessively high pyrolysis temperatures, reducing efficiency. For example, Liu et al. (2015) [66] reported that increasing pyrolysis temperature from 400 °C to 700 °C reduced phosphate removal due to lower surface area.

Recent studies have demonstrated promising performance of advanced modified biochars. Granular iron biochar (GIB) and ball-milled iron biochar (PIB) achieved surface areas of 385 and 331 m^2/g, respectively, and removed phosphate up to 16 times more efficiently than sand filters. PIB

also demonstrated fast adsorption kinetics (0.144 min^{-1}) and suitability for fertiliser reuse [87]. Similarly, ball-milled calcium-loaded biochar (BMCa@BC), synthesised from CaO and corn stover, achieved exceptionally high capacity of 329 mg P/g via hydrogen bonding, complexation, and surface precipitation mechanisms. The recovered phosphate showed high bioavailability (86.7%) and stable performance over five regeneration cycles [88].

These modifications not only increase surface area but also introduce or enhance functional groups that facilitate specific P-binding mechanisms. For example, crawfish-derived biochar pyrolyzed at 600 °C demonstrated P removal via both P adsorption primarily through ion exchange with hydrolysis products ($H_2PO_4^-$, HPO_4^{2-}) and precipitation with dissolved calcium ions [68].

P adsorption increases with increase of temperature of the solution [67,73]. At 25 °C, P primarily showed physical adsorption (bound with biochar as exchangeable P) while at 35 °C chemical adsorption occurred [89]. The value of pH was identified as the most important parameter for adsorption [68–70].

The pH level of the solution significantly influences both the surface charge of the adsorbent and the chemical forms of the contaminant [71,75,76]. The phosphate species present in the solution are different in different pH values, thus affecting the adsorption. $H_3PO_4^{2-}$ is present in lower pH (<2.15), $H_2PO_4^-$ at pH values from 2.15 to 7.20), HPO_4 at neutral to high pH (7.20 to 12.33), and PO_4^{3-} at pH above 12.33 [75]. The adsorption capacity to biochar is typically low at lower pH levels [65,76].

Adsorption of PO_4^{3-} significantly increases the presence of diverse metal elements and availability of functional groups [73,76,90]. However, under certain conditions such as redox or acidic environments, these ions may be released into aqueous solutions, posing potential toxicity to the water environment and aquatic organisms [91].

To enhance adsorption P capacity, biochar is often modified (e.g., with $FeCl_3$, Mg, lanthanide or Ca salts). The LCA accounts and environmental impact associated with the production and use of the biochar adsorbents reach a high price (80–90 $/t), depending on the quality, activation method, and intended market [52].

Modified Agricultural Wastes

Several studies have demonstrated that various agricultural wastes, when chemically modified or iron-loaded, can serve as efficient sorbents for P removal and recovery from wastewater [65,69,70,77]. For instance, walnut and almond shell wastes enhanced with quaternary ammonium groups achieved maximum P adsorption capacities of 22.73 mg/g (modified walnut wooden shells) and 14.71 mg/g (modified almond wooden shells, MAWS) [77]. Under optimal pH conditions (4–5 for MWWS and 4–6 for MAWS), P removal efficiencies improved from 46.25% to 53.5% and from 59.5% to 70.75%, respectively. However, higher pH levels

reduced removal due to diminished electrostatic attraction and increased competition with OH^- ions. Additionally, the spent sorbents could be reused at least four times, ultimately serving as fertilisers to increase plant-available P.

Similarly, the amine cross-linking of spent tea leaves (ACTW) elevated its phosphate removal efficiency and maximum sorption capacity to 98.72 mg/g [65]. Increasing the ACTW dose from 0.4 to 2 g/L raised the phosphate removal from 45.3% to 92.3%, highlighting the influence of sorbent dosage on both adsorption efficiency and the availability of active sites. Both of these modified sorbents rely on electrostatic attraction and ion exchange, emphasising the importance of positively charged functional groups in binding negatively charged phosphate ions.

Iron impregnation further enhances P removal. Iron-loaded lychee (Litchi chinensis) seed wastes, both raw (FeRLW) and charred (FeCLW), achieved maximum adsorption capacities of 96.5 mg/g and 100 mg/g, respectively, within a pH range of 4–6 [70]. Similarly, iron-loaded pomegranate peel (IL-PP) exhibited improved phosphate removal efficiency as pH rose from 3 to 9, increasing from 43.5% to 64.25%. This enhanced performance arises from the greater variety of possible interactions between Fe^{3+} and HPO_4^{2-} at higher pH [69]. The presence of Fe^{2+}/Fe^{3+} provides additional active sites, facilitating robust phosphate capture through both electrostatic attraction and chemisorption mechanisms.

Modifications of agricultural wastes underscore the importance of tailoring adsorbent properties, such as surface chemistry, charge, and functional group density to enhance P uptake. By optimising pH conditions, adjusting sorbent dosage, and selecting appropriate modification techniques, these bio-based materials can achieve high adsorption capacities, maintain efficiency over multiple cycles, and facilitate P recovery for agricultural reuse.

Utilising agricultural and forestry waste (e.g., wood chips, rice husk) avoids landfilling and incineration, resulting in an LCA credit by mitigating associated GHGs and land-use impacts. The major cost driver is the energy used for thermal/chemical activation [92]. The spent, P-saturated agricultural waste material (e.g., wheat straw) is often viewed as a valuable slow-release P fertiliser or soil amendment [93].

Natural Calcium Containing Materials and Calcined Shells

Several studies (Feng et al. (2022) [76], Park et al. (2018) [68], Xu et al. (2023) [75]) indicated that Ca-modified (calcinated) biochar favoured P adsorption. The ability to adsorb P may also be attributed to the adsorbent particle size, pore volume and specific surface [75]. Smaller particle size is usually an indicator for larger specific surface area.

The temperature for production of adsorbent is crucial for later ability for P adsorption. When pyrolysis temperature increased from 700 °C to 900 °C, P adsorption amounts significantly increased [68,73,75,94]. This is

because at 900 °C the amount of calcium is significantly higher than at 700 °C, but the amount of carbon is lower [68]. After pyrolysis at ≤700 °C Ca is in the form of calcite ($CaCO_3$); at 800 °C lime (CaO), portlandite ($Ca(OH)_2$), and calcite; at 900 °C CaO and $Ca(OH)_2$ [71,75]. CaO and $Ca(OH)_2$ are more prone to forming precipitates with P than $CaCO_3$ [68,75]. At higher pyrolysis temperatures the primary mechanism was precipitation between dissolved calcium in CaO and $Ca(OH)_2$ and PO_4^{3-} [68]. Changes in treatment temperature affect the point of zero charge [94].

The adsorption capacity to biochars is typically low at lower pH levels [76]. However, calcined biochars tend to indicate minor decrease in adsorption of P [68,75,76]. This is because calcined biochar has a large amount of Ca(OH)2 on the surface leading to the increase in pH of the solution—due to acid-base neutralisation reaction between the OH^- of $Ca(OH)_2$ and H^+ of the solution. This reaction affects chemical precipitation in phosphate solution with pH < 7 [68,76]. However, an excessive amount of calcium could potentially diminish the adsorption sites available on the adsorbent [75].

In both natural water and wastewater, several common anions have the potential to compete for adsorption sites alongside P. Feng et al. (2022) [76] and Xu et al. (2023) [75] showed that the anions Cl^-, NO^{3-}, and SO_4^{2-} had a minimal impact on the P adsorption. Even at elevated ion concentrations of up to 20 mmol/L for Cl^- and NO_3^-, the P adsorption capacity remained mostly unaffected. However, the presence of HCO_3^- ions had a strong negative effect on the adsorption of P [75,76]. It is hypothesized that CO_3^{2-} reacts with Ca^{2+} from $Ca(OH)_2$ to create a $CaCO_3$ precipitate, which subsequently adheres to the surface, thereby obstructing the phosphate nucleation sites [76].

The material costs on usage of calcined shells as adsorbent is near zero, but the energy cost for calcination must be compared against the savings achieved by avoiding conventional chemicals usage [95]. The unit cost of tertiary P removal using calcined adsorbents remains high, largely due to the elevated temperatures required for pyrolysis during adsorbent preparation [92,95].

Calcium-Doped Materials

Several studies indicate that incorporating calcium often in the form of $Ca(OH)_2$ or $CaCO_3$ into sorbent materials can significantly enhance P removal and facilitate subsequent P recovery. For example, Antunes et al. (2018) [94], Wang et al. (2018) [96], and Pérez et al. (2022) [97] demonstrated that when calcium is incorporated into biochar or biocomposite matrices, it facilitates the formation of stable calcium-phosphate (Ca-P) precipitates such as brushite ($CaHPO_4{\cdot}2H_2O$), monetite ($CaHPO_4$), and/or hydroxyapatite ($Ca_5(PO_4)_3(OH)$), and improves the overall performance in wastewater treatment. Among calcined materials the highest adsorption results were obtained with a Ca-flour biochar

resulting in adsorption capacity of 314.22 mg PO_4/g due to the formation of hydroxyapatite crystal [96].

Bio-based materials and food byproducts offer a sustainable and versatile solution for P removal and recovery from wastewater. Agricultural residues, biosolids, shells, and plant-based wastes can be processed into biochars or modified sorbents that remove P through ion exchange, ligand exchange, complexation, and precipitation [65,69,70,77]. Sorbent performance is often enhanced by metal salt treatments or calcium doping, which facilitate stable Ca-P phase formation and improve efficiency [94,97].

While lab and pilot-scale results are promising, few studies have tested these materials in real wastewater or surface waters [66,72,76]. The limited data available indicate that bio-based sorbents can function effectively under practical conditions, broadening their applicability beyond synthetic solutions. Furthermore, one of the key benefits of bio-based P sorbents lies in their end-of-life valorisation. After adsorption, P-loaded biochars and modified wastes can be applied to soil, enhancing fertility and crop productivity, and reducing dependence on non-renewable phosphate rock [66,72,77].

Utilising Ca-rich waste (e.g., eggshells, oyster shells) assigns the environmental burden to the primary industry, offering an LCA credit and avoiding CO_2 emissions [98]. The cost is competitive against conventional tertiary P removal methods, as the major input is cheap waste material [92]. The dominant economic factor is the energy cost of thermal treatment needed to generate reactive CaO.

The bio-based sorbents, including Ca-doped biochars, modified tea waste, calcined eggshells, are predominantly positioned at TRL 3–4. This category exhibits the highest reported P adsorption capacities across all reviewed materials, with values reaching up to 329 mg P/g for ball-milled Ca-loaded biochar. Despite their high adsorption performance, most investigations remain limited to laboratory-scale proof-of-concept studies using synthetic solutions. Only a small number of studies employed real wastewater matrices such as rural sewage, pond effluent, or agricultural runoff, and these were typically short-term or batch-based rather than sustained pilot-scale operations. Consequently, the absence of long-term field validation and continuous system operation prevents advancement to TRL 5. Current research efforts are primarily focused on improving binding efficiency, regeneration performance, and end-of-life valorisation pathways, particularly the reuse of P-saturated sorbents as soil amendments or slow-release fertilisers.

A comparative overview of bio-based materials, their removal performance, and operating conditions is presented in Table 2.

Table 2. Adsorption of P by bio-based and modified sorbent materials.

Material	Initial concentration, mg/L	Removal efficiency, %	Adsorption capacity, mg/g	Sorption mechanism	Phosphorus medium	TRL level	Ref.
Biochars							
Tea tree biochar	12 mg/L	65%	0.18 mg P/g*	Surface adsorption (Fe-mediated)	Synthetic solution and rainwater	3–4	[63]
Corn straw biochar	1.86–2.47 mg/L	>99%	0.56 mg P/g	Surface adsorption (Fe-mediated)	Synthetic solution and agricultural runoff	3–4	[66]
Soya bean stover biochar	10–200 mg/L	>95%	90.9 mg P/g	Surface Precipitation	Synthetic solution	3–4	[67]
Crawfish biochar	2–240 mg/L	N/A	23.12 mg P/g*	Ion exchange, Ca–P Precipitation	Synthetic solution	3–4	[68]
Eggshells biochar/rice straw biochar 1:1 weight ratio	100 mg/L	N/A	74.06 mg P/g*	Chemisorption	Synthetic solution	3–4	[73]
Eggshells/palm fiber biochars 1:10	200 mg/L	48.30%	72.0 mg P/g	Ligand exchange	Synthetic solution	3–4	[74]
Corn cob, sugarcane bagasse, rice straw, & sawdust biochars	0.5–15 mg/L	16.81% (Corn cob)	N/A	Surface adsorption (monolayer)	Synthetic solution	3–4	[78]
Bagasse biochar	0.3 mg/mL	18% (Fe modified), 40% (La modified), 100% (La/Fe modified)	8.96 mg P/g*	Ligand exchange; Surface precipitation	Synthetic solution	3–4	[78]
Cypress sawdust biochar (600 C)	75 mg/L	66–94%	33.8 mg P/g	Surface adsorption (monolayer)	Synthetic solution	3–4	[83]
Cypress sawdust biochar (magnesium pretreated)	75 mg/L	66–94%	66.7 mg P/g	Surface adsorption (monolayer); Mg–P Precipitation	Synthetic solution	3–4	[83]
Ball-milled Ca-loaded biochar (BMCa@BC) composite	300 mg/L	N/A	329.00 mg P/g (BMCa50)	Electrostatic attraction; Complexation; Ca-P precipitation	Synthetic solution	3–4	[88]
Lychee leaves biochar	10–80 mg/L	N/A	11.62 mg P/g*	Surface precipitation	Synthetic solution	3–4	[89]
Sewage sludge biochar	50 mg/L	N/A	98.97 mg P/g*	Electrostatic Interactions; Ligand exchange	Synthetic solution	3–4	[90]
Calcium-flour biochar (Ca-BC)	100–600 mg/L	N/A	314.22 mg P/g	Ca–P precipitation (apatite formation).	Synthetic solution	3–4	[96]
Modified materials							
Modified tea	50–800 mg/L	45.3%–92.3%	32.19 mg P/g*		Synthetic solution	3–4	[65]

waste				Electrostatic attraction; Ion exchange			
Iron-loaded pomegranate peel	40 mg/L	90%	15.98 mg P/g*	Chemisorption	Synthetic solution	3–4	[69]
Iron-loaded lychee seeds	20 mg/L	~60%	32.61 mg P/g*	Electrostatic attraction	Synthetic solution	3–4	[70]
Lychee seeds	20 mg/L	~30%	31.47 mg P/g*	Surface adsorption (heterogeneous)	Synthetic solution	3–4	[70]
Modified walnut wooden shell (MWWS) and almond wooden shell (MAWS)	5–200 mg/L	64.75%–72%	14.71 mg P/g (MAWS) 22.73 mg P/g (MWWS)	Anion exchange	Synthetic solution	3–4	[77]
Raw materials							
Eggshells	1000 mg/L	N/A	58.24 mg P/g*	Ion exchange; Partial Ca–P precipitation	Synthetic solution	3–4	[71]
Eggshells	0–250 mg/L	N/A	90.80 mg P/g	Ligand exchange; Ca–P precipitation	Synthetic solution	3–4	[97]
Calcined materials							
Calcined eggshells	2.5–500 mg/L	N/A	88.14 mg P/g*	Ca-P Precipitation	Synthetic solution	3–4	[71]
Oyster shell wastes	50–900 mg/L	73.6% (lake water)	228.15 mg P/g	Chemisorption	Synthetic solution and lake water	3–4	[72]
Eggshells + sawdust biochar mix 2:1	100 mg/L	60.20%	301 mg P/g	Chemical adsorption	Synthetic solution and rural domestic sewage	3–4	[75]
Oyster shell + tobacco straw	150 mg/L	91~95%	87 mg P/g	Surface adsorption (monolayer)	Cattle farm wastewater, pond effluent, and domestic sewage	3–4	[76]
Calcium doped							
Calcium-doped biochar (BC20)	100–1500 mg/L	N/A	147 mg P/g	Ca-P Precipitation	Synthetic solution	3–4	[94]
Eggshell/biochar composites with variable $Ca(OH)_2/CaCO_3$ ratio	0–250 mg/L	N/A	134.0 mg P/g	Ligand exchange; Ca–P precipitation (apatite formation)	Synthetic solution	3–4	[97]
Eggshell/biochar composites with variable $Ca(OH)_2/CaCO_3$ ratio	0–250 mg/L	N/A	67.9 mg P/g	Ligand exchange; Ca–P precipitation (apatite formation)	Synthetic solution	3–4	[97]

* Convert to P by multiplying 0.3261.

INDUSTRIAL BY-PRODUCTS FOR P REMOVAL FROM WASTEWATER

Industrial by-products such as slags, ashes, mining residues, and cement-based materials have attracted attention for phosphate removal due to their abundance, low cost, and chemical composition rich in calcium, magnesium, iron, or aluminium oxides. These materials often possess large surface areas, alkaline pH, and reactive functional groups that enable phosphate binding through mechanisms including precipitation, adsorption, ion exchange, and complexation. Their applicability depends not only on sorption capacity but also on factors such as material availability, mechanical stability, pretreatment needs, and potential for P recovery or reuse. While a wide variety of industrial residues have been studied, the most commonly investigated are slags, fly ash, biochar, hydrochar, and bauxite residues. Materials containing organic matter (e.g., sewage sludge, wood waste) are often first pyrolyzed into biochar to improve handling and minimise contaminants. Overall, industrial waste materials represent a promising resource for sustainable P removal, as long as practical limitations such as environmental safety, processing needs, and material longevity are adequately addressed.

Slags

Blast furnace slag, a byproduct of iron production with global output over 1600 million tonnes annually [99], is widely used in concrete production [100]. Due to its alkaline properties and high CaO content (~35%), slag can effectively adsorb phosphate from wastewater, primarily via calcium phosphate (Ca–P) precipitation [101,102]. Although slag's leachability may raise environmental concerns [99], its chemical composition also supports its use in nutrient removal.

Slags are categorised into basic oxygen furnace, blast furnace, and electric arc furnace types, with some variation in CaO, SiO_2, and MgO content [103]. Despite these differences, they are often studied collectively due to similar P removal mechanisms. Numerous studies [101,102,104–106] have confirmed slag's P sorption performance, with Johansson and Gustafsson [102] reporting over 50% of P removed as $CaPO_4$ at a Ca:P molar ratio of 2.9–4. In addition to Ca–P precipitation, adsorption and formation of $CaCO_3$ may also contribute to P removal under high-pH conditions.

Batch tests demonstrated 0.1–0.6 mg P/g capacity with 90–100% removal [102], aligning with Westholm (2010) [105], who observed 25–100% retention in batch and 86–100% in column systems using influent concentrations of 5–25 mg PO_4-P/L. Later studies further explored mechanisms using column setups, indicating that $CaCO_3$ formation at lower pH may reduce adsorption efficiency [101,104,106]. To improve performance, Zhang et al. (2024) [106] mixed slag with rice straw and red soil to form biofilters with lower pH and higher microbial activity, enhancing plant uptake of sorbed P. Similarly, Barca et al. (2014) [101] and Wu et al. (2021) [107] developed composite materials from slag and

expanded silica. These aggregates demonstrated significantly higher P adsorption capacity (4.2 mg/g) due to combined Ca–P precipitation and microporous adsorption, supported by the presence of aluminium in silica. An important operational factor is the slag's age, as younger slag exhibited better P removal and reduced risk of prior leaching [105]. These findings highlight slag's viability for sustainable P removal, particularly when optimised through material combinations or conditioning.

When slags are exposed to air or CO_2 (carbonisation), Ca sequesters CO_2 by forming stable carbonates, offering a net CO_2 reduction benefit to the treatment process, described by Bobicki et al. [108]. Regarding LCA, slag typically requires only minimal treatment, i.e., crushing and sieving, to be utilised as a filter medium. This mechanical treatment has a significantly lower energy and CO_2 footprint compared to the high-temperature thermal activation (calcination or pyrolysis) required for biochar or certain fly ash adsorbents. Costs are restricted almost entirely to collection, crushing, and transportation with costs of typically 10–50 $/t, depending on transport distance. This is significantly lower than virgin commercial adsorbents like granulated activated carbon (1750–6401 $/t) [109].

Oil Shale Ash

The already proven high P-binding capacity of materials containing Ca-, and Al compounds, with a porous structure and alkaline pH, presents an opportunity to study similar materials for such an approach. Such material is also oil shale ash studied by Kaasik et al. [110] and originated as solid waste from burning organic-rich sediment oil-shale in Estonia with annual waste production 5–7 million tonnes [110]. Material is highly calcareous, rich with CaO and $CaSO_4$ and after exposure to environmental conditions and presence of water is also forming hydrated ash containing different secondary Ca-minerals. Similarly to slag also for oils shale ash dominates Ca-P precipitation (both Ca-phosphate and its hydrated form) then following by precipitation of $CaCO_3$, but in hydrated ash there can be recognised also the third phase—reactions of Al in minerals (Ca-(aluminate)-sulphate-hydroxide) [110]. Batch experiments with different particle sizes demonstrated that adsorption on the surface, although existent, still has minor influence on total P sorption capacity. Another aspect similar to slag is lower P sorption with lower used concentration with not clearly trackable sorption mechanism. The opposite is happening for high P concentrations, where removal effectiveness reaches 67–85% and the sorption mechanism can be described using the Freundlich equation. Another study with oil shale ash performed by Kõiv et al. [111] applied in field experiments also confirmed high P retention capacity for systems (vertical and following horizontal filter) filled with oil shale ash (68.9–82.4%), although if using only horizontal filter P retention capacity increases up to 85.4–99.2%. It was found that significantly higher rates of Ca-P precipitation occur when TP concentration in water is above 0.5 mg/L, while in smaller TP concentrations the most probable mechanism for

removal is adsorption [111]. The inconsistency of tracking adsorption in above-mentioned examples and its lower P retention capacity can be explained by competing agents such as organic inhibitors and other ions found in wastewaters.

P binding capacity for hydrated ash sediment has been considered high, up to 65 mg P/g [110,111]. Studies show that incorporating oil shale ash into filters can significantly reduce environmental impact (CO_2, CH_4, and N_2O emissions) compared to traditional filter media (e.g., peat) [112]. Ash is a cost-effective alternative to commercial filter media or the high operational costs associated with conventional chemical precipitation (which requires continuous dosing of expensive chemicals like ferric sulphate or Al-salts). The cost is largely restricted to processing, transport, and filter construction, rather than material costs, being an economic advantage in regions with local ash abundance (e.g., Estonia and Jordan). The spent ash filter material, saturated with Ca-phosphate, can potentially be reused as a P fertiliser source in agriculture, creating a circular economy benefit that offsets the final disposal cost [111].

Fly Ash

Coal combustion by-products, including fly ash and bottom ash, are generated in vast quantities worldwide (~750 million tonnes annually) and have demonstrated potential for P sorption [113]. Xu et al. (2022) [114] reported an adsorption capacity of 1.8 mg P/g for unmodified fly ash, which increased to 10.8 mg P/g after La modification, as the BET surface area increased by a factor of 10.9. This modification also induced the formation of spherical zeolite clusters, shifting the sorption mechanism toward surface adsorption. Further improvements in fly ash performance have been achieved through chemical treatments. Zhou et al. (2019) [113] used sodium dodecyl sulphate (SDS), identifying optimal SDS concentrations of 4% for fly ash and 6% for bottom ash to enhance P uptake by reducing surface tension. In the absence of Ca–P precipitation, sorption mechanisms generally follow Freundlich or Langmuir isotherms.

Fly ash-based composites with lime, clay, or organic amendments have shown improved P capture and structural stability. Li et al. (2017) [115] developed pellets combining fly ash (60%), lime (30%), and clay (10%), achieving high porosity (14%) and P sorption capacity of 1.98 mg/g, with rapid adsorption reaching up to 80% removal within 15–28 min. Sorption was attributed to surface interactions with calcium, iron, and aluminium hydroxides, fitting the Langmuir–Freundlich model. Other hybrid approaches include combining fly ash with woodchips [116] and oyster shells [117]. While P sorption in fly ash–woodchip mixtures was limited under low P concentrations, retention rates were still adequate. In contrast, Jeong et al. (2022) [117] reported a P retention efficiency of 88.4% for oyster shell–fly ash composites over a 120-day period, demonstrating the potential for long-term application. Singh et al. (2022) [118] emphasised fly ash's versatility, not only in P removal but also for

capturing other pollutants in wastewater. Notably, sorption efficiency generally improves with higher initial P concentrations.

The primary environmental benefit of fly ash arises when it displaces energy-intensive manufactured materials, notably Portland cement. LCA highlights that while geopolymer production (a pathway similar to creating high-capacity P adsorbents) avoids massive clinker CO_2 emissions, the production of chemical activators (like Na_2SiO_3) and the energy/heat treatment become the dominant factors determining the final environmental footprint [119]. Some highly effective treatments, such as geopolymer fly ash (GPFA), involve heating the ash/alkali mixture to high temperatures (e.g., 600 °C) [120]. The energy consumed during this thermal step and the CO_2 emitted from the corresponding electricity/fuel consumption represent the major LCA hotspot. Treatment with strong chemicals (e.g., NaOH, HCl) or incorporation of specific metals (e.g., La-modified fly ash, which can reach Qmax of 8.89 mg/g) introduces the environmental impact associated with the production of those chemicals [120]. Utilising fly ash as a supplementary cementitious material (SCM) or geopolymer precursor, which are common pathways for fly ash utilisation, results in a significant reduction of GHG emissions, typically ranging from 42% to 64% compared to OPC production. This saving is attributed to avoiding the high-temperature calcination process (>1500 °C) required for clinker production [119].

Bauxite

Bauxite residue, a by-product of alumina extraction from bauxite ore with global production reaching 150 million tonnes annually, has attracted attention for P sorption due to its high content of Fe_2O_3, Al_2O_3, SiO_2, and CaO [121,122]. Because of its strongly alkaline pH (11–13), various neutralisation techniques have been explored, including gypsum and seawater [123]. Cusack et al. (2018) [122] reported P adsorption capacities of 0.38 mg/g for untreated bauxite residue, 0.48 mg/g with seawater treatment, and 2.46 mg/g using gypsum, with finer particles showing better performance. Among the influencing factors, CaO content exhibited the strongest correlation with P sorption, followed by pH. Barca et al. (2022) [124] confirmed this by using carbonated bauxite residue (CBR), observing increased adsorption from 0.2 to 3.9 mg P/g as initial P concentrations rose from 10 to 200 mg P/L. At low concentrations, P removal occurred through adsorption, while at higher concentrations, calcium phosphate precipitation dominated. Although seawater can adjust pH, its limited availability and the resulting increase in salinity may restrict agricultural reuse [122]. Li et al. (2019) [125] suggested that mixing bauxite residue with organic amendments can mitigate pH and EC fluctuations for soil application.

Red mud, a form of bauxite residue, can be converted through soda sintering into brown mud, a more stable water treatment agent. While red mud exhibits P adsorption up to 7.1 mg/g, some modified forms have

achieved as much as 202.9 mg/g [122,126]. Brown mud has demonstrated even better performance, with sorption capacities reaching 43.1 mg/g [127]. Unlike red mud, brown mud can lower solution pH (2–6), enhancing sorption efficiency. Initially, P adsorption is governed by chemical sorption at low concentrations, shifting toward Ca–P precipitation at higher ones, with the process better described by the Freundlich model [127].

Further development was proposed by Yang et al. (2023) [128], who synthesised a functional biochar (RM-BC) by co-pyrolyzing red mud with walnut shells. The optimised composite reached a maximum P sorption capacity of 15.48 mg/g—higher than either raw red mud or biochar alone. Hematite present in the red mud played a critical role in P removal through Fe–O–P bonding, surface precipitation, and ligand exchange.

The LCA of bauxite residue (BR) use generally finds that the raw material itself has a low environmental cost (often assumed to be 0 kg CO_2 kg) because it is a waste product [108]. However, the CO_2 footprint is generated during the activation necessary to boost its P adsorption capacity from the low capacity of untreated BR (0.2–2.7 mg P/g) to high capacities (50 to 203 mg P/g) achieved through advanced treatment. Raw bauxite cost on adsorbent could be near 0 €/t whereas highly effective treatments (acid or heat/thermal activation up to 700 °C) significantly increase capital and operating expenses, often deemed expensive and energy-consuming [122].

Other Mining-Derived Adsorbent Source

Several mining residues have shown potential for P removal, for example, waste from copper–nickel mining in Botswana. Iron oxide tailings, containing 25.1% Fe_2O_3, and clinker ash, rich in silicon, aluminium, calcium oxides, and SO_3, demonstrated adsorption capacities of 1.29 mg/g and 0.29 mg/g, respectively [127]. XRD analysis confirmed the formation of P-bearing minerals, including $AlPO_4$ and $Mg_2P_2O_7$ in iron tailings, and $Ca_5PO_3(OH)_{13}$ and $FeP(H_4O_6)$ in clinker ash. Interestingly, only the iron tailings facilitated sorption of Ca and Al from wastewater, suggesting greater chemical interaction and potential for regeneration.

Regeneration studies indicated greater durability for iron tailings, with removal efficiencies of 87%, 84%, and 56% across three cycles. In contrast, clinker ash performance dropped more sharply, with efficiencies of 24%, 5%, and 0.6% [129]. Additional research by Christianson et al. (2017) [130] investigated P sorption using iron-rich materials from acid mine drainage, containing 68.4% Fe_2O_3. Column experiments with low P concentrations (1.39 ± 0.22 mg P/L) showed 58% retention within hours and up to 98% retention after 51 h, with potential for regeneration using 0.5 M NaOH. Similarly, Dobbie et al. (2009) [131] reported that hydrous iron oxides, despite a lower adsorption capacity of 0.065 mg/g, exhibited an estimated lifespan up to ten times longer than other tested sorbents.

Magnesite production waste, rich in magnesium oxide and typically collected through electrostatic separation, achieved removal efficiencies of up to 96% under high P concentrations and extended contact times after calcination, which reduced mass by 42 to 45%. At lower dosages, removal efficiency fell below 65%, whereas a concentration of 1 g/L facilitated struvite precipitation, identified as the dominant P removal mechanism [132]. The precipitation of struvite ($MgNH_4PO_4$ $6H_2O$) is a highly efficient method for PO_4 recovery, which accounts for approximately 85% of the total P content in the source material. Nättorp et al. [133] determining the specific recovery cost to be in the range of 4 to 10 €/kg of recovered P.

Alum sludge, a by-product of water treatment plants, has also been explored as a sorbent. Duranceau and Biscardi (2015) [134] tested dried alum sludge in column experiments with surface water containing less than 200 µg P/L, achieving an adsorption capacity of 6.94 mg/g and 51% retention. Similarly, Babatunde and Zhao (2010) [135] reported adsorption capacities ranging from 10.2 to 31.9 mg/g, highest at pH 4, and confirmed that sorption followed the Langmuir model. Minor aluminium leaching was observed during the initial three weeks. The mechanism was attributed to surface exchange reactions, followed by other interactions once functional sites were saturated.

Industrial Waste Products

Industrial waste materials rich in calcium, such as dolomite powder generated during quarry processing (blasting, grinding, and sieving) and concrete waste, have been explored for P removal. Dolomite powder exhibited relatively low sorption capacity (0.025–0.072 g PO_4/g), which improved with higher P concentrations and longer contact time. Regeneration was possible using water or weak acids, though strong acids caused material loss [136]. Cement-based materials demonstrated high P removal efficiency, with cement mortar achieving up to 10.1 mg P/g (30.96 mg PO_4/g) and over 94% removal across a wide concentration range. Their sorption capacity correlated positively with the total content of Al_2O_3, Fe_2O_3, and CaO, and was primarily attributed to precipitation mechanisms, complemented by weak physical interactions [137]. In addition, Egemose et al. (2012) [138] highlighted the applicability of these materials in systems like sedimentation ponds and subsurface flow treatments.

One of the main challenges in using Ca-based materials is their tendency to raise the initial pH of treated water up to 12, which, while enhancing P retention, leads to a significant decline in efficiency as the pH decreases. Additionally, the high variability in composition and particle size among different material types complicates their standardisation and consistent performance [137].

A comparative overview of industrial by-products, their removal performance, and operating conditions is presented in Table 3.

Table 3. Adsorption of P by industrial by-products and modified waste-derived sorbents.

Material	Initial concentration, mg/L	Removal efficiency, %	Adsorption capacity, mg/g	Sorption mechanism	Phosphorus medium	TRL level	Ref.
Slags							
Slag	10.82 ± 1.01 mg/L (9.04–12.43 mg/L)	>88% (P) >91% (PO_4-P)	0.91–1.05 mg P/g	Ca-Precipitation	Synthetic solution	3–4	[101]
Blast furnace slag	5–25 mg/L	90–100% laboratory, 40–53% field	0.1–0.6 mg P/g	Ca-P precipitation	Synthetic solution	3–4	[102]
Basic oxygen furnace and blast furnace steel slags	0.06 mg/L	~90% that decreased over time to 40%	-	-	Tile drainage water and agricultural runoff	5–6	[104]
Slag	0.17–0.30 mg/L	55–81%	12.28 mg P/g	Ca/Fe/Al–P Precipitation	Simulated wastewater	3–4	[106]
Slag with porous expanded silica	168 mg/L	100%/24h	4.2 mg P/g	Ca-P precipitation; micropore adsorption	Synthetic solution	3–4	[107]
Oil shale ash							
Oil-shale ash	326 mg/L	67–85%	1.0–4.0 mg P/g (small conc.) ≤65 (high conc.)	Ca-P precipitation; Surface adsorption (heterogeneous sites)	Synthetic solution	3–4	[110]
Hydrated oil shale ash	0.13–17.0 mg/L	68.9–82.4% (vertical + horizontal), 85.4–99.2% (horizontal filter)	-	Ca-P precipitation	Pre-treated municipal wastewater and landfill leachate	5–6	[111]
Fly ash							
Fly ash	0.5–100 mg/L	58%	2.05 mg P/g*	Ca-P precipitation; Surface adsorption (heterogeneous sites)	Synthetic and primary municipal wastewater influent	3–4	[113]
Bottom ash	0.5–100 mg/L	69%	2.56 mg P/g	Surface adsorption (monolayer)	Synthetic and primary municipal wastewater influent	3–4	[113]
Fly ash	10–30 mg/L	72.80%	10.8 mg P/g	-	Synthetic solution and lake water	3–4	[114]
Fly ash	1.0 mg/L	80%	1.98 mg P/g	Surface adsorption (heterogeneous monolayer)	Synthetic solution	3–4	[115]
Fly ash	5 mg/L	81.7–84.5%	0.059–0.114 mg P/g	Surface ion exchange (Ca/Fe/Al hydroxides)	Subsurface drainage outflow	3–4	[116]
Bottom ash	1.55 mg/L	88.40%	$8.24*10^{-5}$ mg P/g (from sediments)	-	Eutrophic coastal sediments	3–4	[117]
Bauxite							
Bauxite residue	-	-	1.39–2.73 mg P/g	Surface adsorption (monolayer)	Synthetic solution	3–4	[122]

Carbonated bauxite residues (CBR)	10–200 mg/L	87-97%	0.2 to 3.9 mg P/g	Surface adsorption; Ca-P Precipitation	Wastewater	3–4	[124]
Bauxite residue	1.5–800 mg/L	37% (red mud);	17.0 mg P/g (red mud);	Surface adsorption (heterogeneous sites)	Synthetic solution	3–4	[127]
		55% (brown mud)	43.1 mg P/g (brown mud)				
Iron oxide tailings	21.3 mg/L	98%	1.29 mg P/g	Surface adsorption (monolayer)	Tertiary wastewater effluent	3–4	[127]
Red mud (RM) and low-cost walnut shell biochar	-	-	15.48 mg P/g	Surface precipitation; Ligand exchange	Synthetic solution	3–4	[128]
Mine drainage residue (iron rich)	1.39 ± 0.22 mg/L	98% (51h)	2.43 mg P/g	-	Aquaculture effluent (P with NO_3^-)	5–6	[130]
Other mining-derived adsorbent source							
Clinker waste	21.3 mg/L	37%	0.29 mg P/g	Surface adsorption (monolayer)	Tertiary wastewater effluent	3–4	[129]
Magnesite dust	216.85 mg/L	75–96%	-	Struvite precipitation (high conc.)	Synthetic and liquid digestate	3–4	[132]
Dried alum sludge	0.05–0.1 mg/L	51%	6.94 mg P/g*	Surface adsorption (monolayer)	River water	3–4	[134]
Alum sludge	0–360 mg/L	-	31.9 mg P/g	Surface adsorption (monolayer)	Synthetic solution	3–4	[135]
Raw dolomite powder	0.09–0.11 mg/L	-	0.008–0.023 mg P/g	Surface adsorption (monolayer)	Synthetic groundwater, tap water, secondary treated wastewater	3–4	[136]
Cement-based mortar	0–1000 mg/L	≤94%	10.1 mg P/g	Ca/Fe/Al–P Precipitation	Synthetic wastewater	3–4	[137]
Crushed concrete	1 g/L	≤98%	5.1–19.6 mg P/g	Surface adsorption (monolayer)	Synthetic solution	3–4	[138]

* Convert to P by multiplying 0.3261.

Industrial by-products presented exhibit the widest range of technology maturity, spanning from TRL 3–4 to TRL 5–6. While many materials such as fly ash, bauxite residue, crushed concrete, and alum sludge remain at TRL 3–4 due to laboratory-scale evaluation, several Ca- and Fe-rich residues have progressed to higher maturity levels. Specifically, steel slags, oil shale ash, and mine drainage residues have reached TRL 5–6 through validation in pilot-scale or field-based systems operated with real wastewater or drainage flows. Steel slags have been tested under agricultural runoff and tile drainage conditions, oil shale ash has demonstrated high P retention in vertical and horizontal filter systems treating municipal wastewater and landfill leachate, and Fe-rich mine drainage residues combined with woodchips have shown stable performance during extended aquaculture effluent treatment. These materials are considered more technologically mature because they have been evaluated under operationally relevant conditions, demonstrating feasibility for scale-up despite variability in long-term performance. However, further advancement toward widespread WWTP integration is constrained by material heterogeneity, environmental safety considerations, and standardisation requirements.

CONCLUSIONS

This comprehensive review highlights the potential of sustainable sorbent materials for P removal and recovery from wastewater, focusing on three major categories: mineral-based sorbents, bio-based materials, and industrial by-products. Comparative analysis shows that bio-based sorbents, particularly calcium-doped biochars derived from biosolids or agro-waste, achieve the highest adsorption capacities, reaching up to 329 mg P/g. Mineral-based materials demonstrate intermediate performance (0.07–152.1 mg P/g), while industrial by-products such as fly ash and slags show more variable but generally lower capacities (8.2×10^{-5} to 43.1 mg P/g), depending on composition and treatment.

The observed pattern: bio-based > mineral-based > industrial, emphasises the importance of material origin and surface modification in determining P uptake. Across all sorbent types, key mechanisms include ion exchange, ligand exchange, and precipitation, often facilitated by doping with metals like Ca, Fe, La, or Zr to enhance active site availability and support the formation of stable calcium-phosphate compounds (e.g., brushite, hydroxyapatite).

Regeneration and reuse remain central to long-term sustainability. Several materials, such as La or Fe-modified biochars and Ca-loaded composites, have been successfully regenerated and reused up to ten times without significant performance loss. Moreover, many bio-based sorbents offer post-use value as soil amendments, aligning with circular economy goals and reducing reliance on mined phosphate rock.

While bio-based materials are often low-cost and renewable, mineral-based sorbents may require energy-intensive synthesis, and industrial by-products may demand pre-treatment due to heterogeneity. Additionally, sorption efficiency for industrial materials often correlates with longer contact times and higher P concentrations, limiting their versatility in wastewaters with limited P content.

Despite promising laboratory-scale results, most emerging sorbents remain below TRL 6 due to the limited evidence of long-term validation under real wastewater and operationally relevant conditions. Additional constraints include the lack of standardised testing and reporting protocols, as well as insufficiently demonstrated regeneration and P recovery or reuse pathways. Furthermore, the integration of these materials into existing wastewater treatment trains, together with alignment to regulatory requirements, remains a key challenge for large-scale implementation and technology adoption.

To accelerate the development and deployment of effective P sorbents, future research should prioritise:

1. Develop advanced materials with higher P binding efficiency to meet stricter discharge regulations and address diverse wastewater conditions.
2. Investigate cost-effective and environmentally friendly methods for sorbent regeneration and reuse to reduce operational costs.
3. Leverage industrial and agricultural by-products to create low-cost, high-performance sorbents, promoting circular economy principles.
4. Combine emerging technologies with established ones for comprehensive wastewater treatment and nutrient recovery solutions.
5. Align research priorities with regulatory frameworks and foster collaborations with policymakers to accelerate adoption.

A multidisciplinary approach that combines material science, process engineering, environmental policy, and socio-economic analysis is essential to implement these innovations into scalable and practical solutions for sustainable P management.

SUPPLEMENTARY MATERIALS

The following supplementary materials are available online, Figure S1: PRISMA flow diagram of the literature search and study selection process.

DATA AVAILABILITY

All data generated in the study are available in the manuscript or supplementary files.

AUTHOR CONTRIBUTIONS

Conceptualisation, RO-D and KG; formal analysis, KG, AK and JK; methodology, RO-D and KG; writing-original draft, RO-D, KG, OP, AK and SK; writing-review and editing, IZ, JK and SO-G; visualisation, SO-G and JK; supervision, IZ and AK. All authors have read and agreed to the published version of the manuscript.

CONFLICTS OF INTEREST

The authors declare that they have no conflict of interest.

FUNDING

This work was supported by LCS FARP project “Unused Latvia’s natural mineral resources for the development of innovative composite materials for phosphorus recovery from small municipal and industrial wastewater treatment plants to implement the principles of circular economy [CircleP, No. lzp-2021/1-0090]”, Interreg Estonia-Latvia programme project “Circular Nutrient Recovery for Sustainable Municipalities [NutriLoopWorks, EE-LV00163]” and Interreg Central Baltic programme project “Reuse of Nutrients and Water from Human based sludge” [ReNuW-Hubs, CB0700318]. Ruta Ozola-Davidane’s and Andrejs Krauklis’ contributions were supported by TEN4 project “Allocation of state budget funding for tenure professorship to the Latvia University of Life Sciences and Technologies for 2024”. Ivar Zekker was supported by EIC for “Reduction of greenhouse gas emissions in the wastewater treatment sector by autotrophic nitrogen removal as an alternative to heterotrophic processes”, “The reuse/recycling of textile waste as a biomass carrier material for the removal and recycling of organic pollutants and heavy metals from wastewater, excess sludge, compost, and ash using biological methods” and by NEUTEN MSCA fellowships, and further COST actions: CA20101, CA20127, CA20138, CA22102, CA22110, CA22123, CA22162, and CA22146.

ACKNOWLEDGMENTS

Authors are greatly thankful to Diana Mikanova who made the artwork for the graphical abstract.

REFERENCES

1. Li X, Liu Y, Su L, Lei X. Adsorption properties of modified eggshell on phosphorus in water. E3S Web Conf. 2021;252:03050. doi: 10.1051/e3sconf/202125203050
2. Kalaitzidou K, Mitrakas M, Zouboulis A. Post-removal of phosphorus from biologically treated wastewater and recovering it as fertilizer: Pilot-scale attempt–Project Phorese. Water. 2024;16(11):1527. doi: 10.3390/w16111527

3. Anders A, Weigand H, Platen H. Phosphorus recovery by re-dissolution from activated sludge—effects of carbon source and supplementation level revisited. Environ Sci Water Res Technol. 2023;9(1):134–45. doi: 10.1039/d2ew00356b
4. Mao Y, Xiong R, Gao X, Jiang L, Peng Y, Xue Y. Analysis of the status and improvement of microalgal phosphorus removal from municipal wastewater. Processes. 2021;9(9):1486. doi: 10.3390/pr9091486
5. Šarko J, Mažeikienė A. Investigation of sorbents for phosphorus removal, in: Environmental Engineering. Proceedings of the 1st International Conference on Environmental Engineering (ICEE); 2020 May 21-22; Vilnius, Lithuania. doi: 10.3846/enviro.2020.620
6. Witek-Krowiak A, GorazdaK, Szopa D, Trzaska K, Moustakas K, Chojnacka K. Phosphorus recovery from wastewater and bio-based waste: An overview. Bioengineered. 2022;13(5):13474-506. doi: 10.1080/21655979.2022.2077894
7. Mažeikienė A, Šarko J. Removal of nitrogen and phosphorus from wastewater using layered filter media, Sustainability. 2022;14(17):10713. doi: 10.3390/su141710713
8. Ramlogan M, Rabinovich A, Rouff A. Thermochemical analysis of ammonia gas sorption by struvite from livestock wastes and comparison with biochar and metal–organic framework sorbents. Environ Sci Technol. 2020;54(20):13264-73. doi: 10.1021/acs.est.0c02572
9. Shabtai I, Mishael Y. Polycyclodextrin–clay composites: Regenerable dual-site sorbents for bisphenol A removal from treated wastewater. ACS Appl Mater Interfaces. 2018;10(32):27088-97. doi: 10.1021/acsami.8b09715
10. Kondratenko A, Buyantuev S. On the issue of wastewater treatment with an organomineral sorbent obtained by electroplasmic processing of coal flotation tailings. IOP Conf Ser Earth Environ Sci. 2022;1070(1):012036. doi: 10.1088/1755-1315/1070/1/012036
11. Rozumová L, Legátová B, Prehradná J. Potential of the biosorbent from waste for the separation of Cu(II) from aqueous solutions. Key Eng Mater. 2018;779:102-9. doi: 10.4028/www.scientific.net/kem.779.102
12. Adrah K. Mechanistic understanding of sieving lithium ions using a biobased sorbent technology for sustainable lithium reclamation and cleansing brines. ACS Omega. 2024;9(26):28091-103. doi: 10.1021/acsomega.3c09716
13. Alvarado S, Megia-Fernandez A, Ortega-Muñoz M, Hernández-Matéo F, Lopéz-Jaramillo J, Santoyo-González F. Removal of the water pollutant ciprofloxacin using biodegradable sorbent polymers obtained from polysaccharides. Polymers. 2023;15(15):3188. doi: 10.3390/polym15153188
14. Osman A, El-Monaem E, Elgarahy A, Aniagor C, Hosny M, Farghali M, et al. Methods to prepare biosorbents and magnetic sorbents for water treatment: A review. Environ Chem Lett. 2023;21(4):2337-98. doi: 10.1007/s10311-023-01603-4
15. Patel H, Routoula E. Patwardhan S, Decontamination of anthraquinone dyes polluted water using bioinspired silica as a sustainable sorbent. Silicon. 2021;14(3):1235-45. doi: 10.1007/s12633-020-00851-1

16. Paulauskienė T, Uebe J, Ziogas M. Cellulose aerogel composites as oil sorbents and their regeneration. PeerJ. 2021;9:e11795. doi: 10.7717/peerj.11795
17. Sheard W, Park K, Leitao E. Polysulfides as sorbents in support of sustainable recycling. ACS Sustain Chem Eng. 2023;11(9):3557-67. doi: 10.1021/acssuschemeng.2c07386
18. Xu C, Strömme M. Sustainable porous carbon materials derived from wood-based biopolymers for CO_2 capture. Nanomaterials. 2019;9(1):103. doi: 10.3390/nano9010103
19. Page MJ, McKenzie JE, Bossuyt PM, Boutron I, Hoffmann TC, Mulrow CD, et al. The PRISMA 2020 statement: An updated guideline for reporting systematic reviews. BMJ. 2021;372:71. doi: 10.1136/bmj.n71
20. Azizian N, Mazzuchi T, Sarkani S, Rico D. A framework for evaluating technology readiness, system quality, and program performance of U.S. DoD acquisitions. Syst Eng. 2011;14(4):410-26. doi: 10.1002/sys.20186
21. Kedia S, Baker J, Carbonell R, Lee K, Roberts C, Erickson J, Pluschkell S. Biomanufacturing readiness levels (BRL)—A shared vocabulary for biopharmaceutical technology development and commercialization. Biotechnol Bioeng. 2022;119(12):3526-36. doi: 10.1002/bit.28227
22. Yfanti S, Sakkas N. Technology readiness levels (TRLs) in the era of co-creation. Appl Syst Innov. 2024;7(2):32. doi: 10.3390/asi7020032
23. Buchner G, Stepputat K, Zimmermann A, Schomäcker R. Specifying technology readiness levels for the chemical industry. Ind Eng Chem Res. 2019;58(17):6957-69. doi: 10.1021/acs.iecr.8b05693
24. European Commission. Horizon Europe Work Programme 2025: 14. General Annexes. Brussels (Belgium): European Commission, (2025). Available from: https://research-and-innovation.ec.europa.eu/document/download/9d9a75d4-6da8-4902-95c4-34a4de01ebe5_en. Accessed on 2025 Dec 20.
25. Abdoli S, Asgari Lajayer B, Dehghanian Z, Bagheri N, Vafaei AH, Chamani M, et al. A review of the efficiency of phosphorus removal and recovery from wastewater by physicochemical and biological processes: Challenges and opportunities. Water. 2024;16(17):2507. doi: 10.3390/w16172507
26. Xie J, Wang Z, Fang D, Li C, Wu D. Green synthesis of a novel hybrid sorbent of zeolite/lanthanum hydroxide and its application in the removal and recovery of phosphate from water. J Colloid Interface Sci. 2014;423:13-9. doi: 10.1016/j.jcis.2014.02.020
27. He Y, Lin H, Dong Y, Liu Q, Wang L. Simultaneous removal of ammonium and phosphate by alkaline-activated and lanthanum-impregnated zeolite. Chemosphere. 2016;164:387-95. doi: 10.1016/j.chemosphere.2016.08.110
28. Kong L, Tian Y, Li N, Liu Y, Zhang J, Zuo W. Highly-effective phosphate removal from aqueous solutions by calcined nano-porous palygorskite matrix with embedded lanthanum hydroxide. Appl Clay Sci. 2018;162:507-17. doi: 10.1016/j.clay.2018.07.005

29. Kasprzyk M, Gajewska M. Phosphorus removal by application of natural and semi-natural materials for possible recovery according to assumptions of circular economy and closed circuit of P. Sci Total Environ. 2019;650:249-56. doi: 10.1016/j.scitotenv.2018.09.034
30. Karthikeyan P, Thagira Banu HA, Meenakshi S. Removal of phosphate and nitrate ions from aqueous solution using La^{3+} incorporated chitosan biopolymeric matrix membrane. Int J Biol Macromol. 2019;124:492-504. doi: 10.1016/j.ijbiomac.2018.11.127
31. Shi W, Fu Y, Jiang W, Ye Y, Kang J, Liu D, et al. Enhanced phosphate removal by zeolite loaded with Mg–Al–La ternary (hydr)oxides from aqueous solutions: Performance and mechanism. Chem Eng J. 2019;357:33-44. doi: 10.1016/j.cej.2018.08.003
32. Wei T, Zhang G, Long Z, Xian G, Niu L. Advanced phosphate removal by La–Zr–Zn ternary oxide: Performance and mechanism. J Alloys Compd. 2020;817:152745. doi: 10.1016/j.jallcom.2019.152745
33. Luo Q, Wei J, Guo Z, Song Y. Adsorption and immobilization of phosphorus from water and sediments using a lanthanum-modified natural zeolite: Performance, mechanism and effect. Sep Purif Technol. 2024;329:125187. doi: 10.1016/j.seppur.2023.125187
34. Haque N, Hughes A, Lim S, Vernon C. Rare Earth Elements: Overview of Mining, Mineralogy, Uses, Sustainability and Environmental Impact. Resources. 2014;3:614-35. doi: 10.3390/resources3040614
35. Drenkova-Tuhtan A, Schneider M, Franzreb M, Meyer C, Gellermann C, Sextl G, et al. Pilot-scale removal and recovery of dissolved phosphate from secondary wastewater effluents with reusable ZnFeZr adsorbent@Fe_3O_4/SiO_2 particles with magnetic harvesting. Water Res. 2017;109:77-87. doi: 10.1016/j.watres.2016.11.039
36. Li J, Li B, Yu W, Huang H, Han JC, Huang Y, et al. Lanthanum-based adsorbents for phosphate reutilization: Interference factors, adsorbent regeneration, and research gaps. Sustain Horiz. 2022;1:100011. doi: 10.1016/j.horiz.2022.100011
37. Nguyen TAH, Ngo HH, Guo WS, Pham TQ, Li FM, Nguyen TV, et al. Adsorption of phosphate from aqueous solutions and sewage using zirconium loaded okara (ZLO): Fixed-bed column study. Sci. Total Environ. 2015;523:40-9. doi: 10.1016/j.scitotenv.2015.03.126
38. Huang W, Chen J, He F, Tang J, Li D, Zhu Y, et al. Effective phosphate adsorption by Zr/Al-pillared montmorillonite: Insight into equilibrium, kinetics and thermodynamics. Appl. Clay Sci. 2015;104:252-60. doi: 10.1016/j.clay.2014.12.002
39. Johir MAH, Pradhan M, Loganathan P, Kandasamy J, Vigneswaran S. Phosphate adsorption from wastewater using zirconium (IV) hydroxide: Kinetics, thermodynamics and membrane filtration adsorption hybrid system studies. J Environ Manag. 2016;167:167-74. doi: 10.1016/j.jenvman.2015.11.048

40. Xiong W, Tong J, Yang Z, Zeng G, Zhou Y, Wang D, et al. Adsorption of phosphate from aqueous solution using iron–zirconium modified activated carbon nanofiber: Performance and mechanism. J Colloid Interface Sci. 2017;493:17-23. doi: 10.1016/j.jcis.2017.01.024
41. Kumar IA, Viswanathan N. Development of multivalent metal ions imprinted chitosan biocomposites for phosphate sorption. Int J Biol Macromol. 2017;104:1539-47. doi: 10.1016/j.ijbiomac.2017.02.100
42. Zeng G, Li G, Wu Y, Tang C, Yuan W, Zhong H, et al. Preparation of high specific surface area Zn/Al/Zr LDH@HTCC for enrichment and recovery of phosphorus from water. Surf Interfaces. 2023;42:103330. doi: 10.1016/j.surfin.2023.103330
43. Nuss P, Eckelman MJ. Life cycle assessment of metals: A scientific synthesis. PLOS ONE. 2014;9(7):e101298. doi: 10.1371/journal.pone.0101298
44. Song J, Fan J, Liu J, Liu R, Qu J, Qi T. A two-step zircon decomposition method to produce zirconium oxychloride: alkali fusion and water leaching. Rare Met. 2015;39(4):448-54. doi: 10.1007/s12598-015-0537-y
45. Sleiman N, Deluchat V, Wazne M, Mallet M, Courtin-Nomade A, Kazpard V, et al. Phosphate removal from aqueous solution using ZVI/sand bed reactor: Behavior and mechanism. Water Res. 2016;99:56-65. doi: 10.1016/j.watres.2016.04.054
46. Zavareh D, Behrouzi Z, Avanes A. Cu(II) binded chitosan/Fe_3O_4 nanocomposite as a new biosorbent for efficient and selective removal of phosphate. Int J Biol Macromol. 2017;101:40-50. doi: 10.1016/j.ijbiomac.2017.03.074
47. Gu W, Xie Q, Xing M, Wu D. Enhanced adsorption of phosphate onto zinc ferrite by incorporating cerium. Chem Eng Res Des. 2017;117:706-14. doi: 10.1016/j.cherd.2016.11.026
48. Guaya D, Jiménez R, Sarango J, Valderrama C, Cortina JL. Iron-doped natural clays: Low-cost inorganic adsorbents for phosphate recovering from simulated urban treated wastewater. J Water Process Eng. 2021;43:102274. doi: 10.1016/j.jwpe.2021.102274
49. Kong X, Bai R, Wang S, Wu B, Zhang R, Li H. Recovery of phosphorus from aqueous solution by magnetic TiO_2*/Fe_3O_4 composites. Chem Phys Lett. 2022;787:139234. doi: 10.1016/j.cplett.2021.139234
50. Tan X, Yi L, Duan Z, Wu X, Ali I, Gao L. Phosphorus recovery from wastewater using extracellular polymeric substances (EPS)-like hydrogels. J Water Process Eng. 2023;52:103512. doi: 10.1016/j.jwpe.2023.103512.
51. Xiao X, Liu S, Zhang X, Zheng S. Phosphorus removal and recovery from secondary effluent in sewage treatment plant by magnetite mineral microparticles. Powder Technol. 2017;306:68-73. doi: 10.1016/j.powtec.2016.10.066
52. Feng H, Yang F, Wei C. Developing goethite modified reed-straw biochar for remediation of metal(loids) co-contamination. Colloids Surf A Physicochem Eng Asp. 2024;692:133942. doi: 10.1016/j.colsurfa.2024.133942

53. Alshameri A, Yan C, Lei X. Enhancement of phosphate removal from water by TiO_2/Yemeni natural zeolite: Preparation, characterization and thermodynamic. Micropor Mesopor Mater. 2014;196:145-7. doi: 10.1016/j.micromeso.2014.05.008
54. Shams M, Dehghani MH, Nabizadeh R, Mesdaghinia A, Alimohammadi A, Najafpoor AA. Adsorption of phosphorus from aqueous solution by cubic zeolitic imidazolate framework-8: Modeling, mechanical agitation versus sonication. J Mol Liq. 2016;224:151-7. doi: 10.1016/j.molliq.2016.09.059
55. Zhu W, Wang R, Tang Q, Zhang Z, Yin Z, Yang Z, et al. Renewable adsorbents for selective phosphorus removal: $Co(OH)_2$-derived ZIF-67 on anion exchange resin. Langmuir. 2023;39(25):8760-8. doi: 10.1021/acs.langmuir.3c00752
56. Mitrogiannis D, Psychoyou M, Koukouzas N, Tsoukalas N, Palles D, Kamitsos E, et al. Phosphate recovery from real fresh urine by $Ca(OH)_2$ treated natural zeolite. Chem Eng J. 2018;347:618-30. doi: 10.1016/j.cej.2018.04.102
57. Lu Z, Zhang K, Liu F, Gao X, Zhai Z, Li J, et al. Simultaneous recovery of ammonium and phosphate from aqueous solutions using Mg/Fe modified NaY zeolite: Integration between adsorption and struvite precipitation. Sep Purif Technol. 2022;299:121713. doi: 10.1016/j.seppur.2022.121713
58. Yan H, Chen Q, Liu J, Feng Y, Shih K. Phosphorus recovery through adsorption by layered double hydroxide nano-composites and transfer into a struvite-like fertilizer. Water Res. 2018;145:721-30. doi: 10.1016/j.watres.2018.09.005
59. Yang F, Zhang S, Sun YCW, Tsang DCW, Cheng K, Ok YS. Assembling biochar with various layered double hydroxides for enhancement of phosphorus recovery. J Hazard Mater. 2019;365:665-73. doi: 10.1016/j.jhazmat.2018.11.047
60. Zhang J, Huang W, Yang D, Xiang J, Chen Y. Removal and recovery of phosphorus from secondary effluent using layered double hydroxide–biochar composites. Sci Total Environ. 2022;844:156802. doi: 10.1016/j.scitotenv.2022.156802
61. Xavier GTM, Urzedo AL, Nunes RS, Fadini PS, Carvalho WA. Incorporation of clay-based adsorbent into polyvinylidene fluoride membrane for enhanced phosphorus capture in aqueous solution. Resour Conserv Recycl. 2023;190:106867. doi: 10.1016/j.resconrec.2023.106867
62. Li Z, Wang L, Meng J, Liu X, Xu J, Wang F, Brookes P. Zeolite-supported nanoscale zero-valent iron: New findings on simultaneous adsorption of Cd(II), Pb(II), and As(III) in aqueous solution and soil. J Hazard Mater. 2018;344:1-11. doi: 10.1016/j.jhazmat.2017.09.036
63. Gubernat S, Masłoń A, Czarnota J, Koszelnik P. Phosphorus removal from wastewater using marl and travertine and their thermal modifications. Desal Water Treat. 2022;275:35-46. doi: 10.5004/dwt.2022.28529
64. Salimova A, Zuo J, Liu F, Wang Y, Wang S, Verichev K. Ammonia and phosphorus removal from agricultural runoff using cash crop waste-derived biochars. Front Environ Sci Eng. 2020;14:48. doi: 10.1007/s11783-020-1225-1
65. Qiao H, Mei L, Chen G, Liu H, Peng C, Ke F, et al. Adsorption of nitrate and phosphate from aqueous solution using amine cross-linked tea wastes. Appl Surf Sci. 2019;483:114-22. doi: 10.1016/j.apsusc.2019.03.147

66. Liu F, Zuo J, Chi T, Wang P, Yang B. Removing phosphorus from aqueous solutions by using iron-modified corn straw biochar. Front Environ Sci Eng. 2015;9:1066-75. doi: 10.1007/s11783-015-0769-y
67. Karunanithi R, Ok YS, Dharmarajan R, Ahmad M, Seshadri B, Bolan N, et al. Sorption, kinetics and thermodynamics of phosphate sorption onto soybean stover derived biochar. Environ Technol Innov. 2017;8:113-25. doi: 10.1016/j.eti.2017.06.002
68. Park JH, Wang JJ, Xiao R, Zhou B, Delaune RD, Seo DC. Effect of pyrolysis temperature on phosphate adsorption characteristics and mechanisms of crawfish char. J Colloid Interface Sci. 2018;525:143-51. doi: 10.1016/j.jcis.2018.04.078
69. Bellahsen N, Kakuk B, Beszédes S, Bagi Z, Halyag N, Gyulavári T, et al. Iron-loaded pomegranate peel as a bio-adsorbent for phosphate removal. Water. 2021;13(19):2709. doi: 10.3390/w13192709
70. Shrestha A, Poudel BR, Silwal M, Pokhrel MR. Adsorptive removal of phosphate onto iron-loaded Litchi chinensis seed waste. J Inst Sci Technol. 2019;23(1):81-7. doi: 10.3126/jist.v23i1.22200
71. Park JH, Choi AY, Lee SL, Lee JH, Rho JS, Kim SH, et al. Removal of phosphates using eggshells and calcined eggshells in high phosphate solutions. Appl Biol hem. 2022;65:75. doi: 10.1186/s13765-022-00744-4
72. Lee JI, Kang JK, Oh JS, Yoo SC, Lee CG, Jho EH, et al. New insight to the use of oyster shell for removing phosphorus from aqueous solutions and fertilizing rice growth. J Clean Prod. 2021;328:129536. doi: 10.1016/j.jclepro.2021.129536
73. Liu X, Shen F, Qi X. Adsorption recovery of phosphate from aqueous solution by CaO-biochar composites prepared from eggshell and rice straw. Sci Total Environ. 2019;666:694-702. doi: 10.1016/j.scitotenv.2019.02.227
74. Pérez S, Muñoz-Saldaña J, Acelas N, Flórez E. Phosphate removal from aqueous solutions by heat treatment of eggshell and palm fiber. J Environ Chem Eng. 2021;9(1):104684. doi: 10.1016/j.jece.2020.104684
75. Xu C, Liu R, Tang Q, Hou Y, Chen L, Wang Q. Adsorption removal of phosphate from rural domestic sewage by Ca-modified biochar derived from waste eggshell and sawdust. Water. 2023;15(17):3087. doi: 10.3390/w15173087
76. Feng M, Li M, Zhang L, Luo Y, Zhao D, Yuan M, et al. Oyster shell modified tobacco straw biochar: Efficient phosphate adsorption at wide range of pH values. Int J Environ Res Public Health. 2022;19(12):7227. doi: 10.3390/ijerph19127227
77. Faraji B, Zarabi M, Kolahchi Z. Phosphorus removal from aqueous solution using modified walnut and almond wooden shell and recycling as soil amendment, Environ. Monit. Assess. 2020;192:373. doi: 10.1007/s10661-020-08326-x.
78. Yi Y, Fu Y, Wang Y, Xu Z, Diao Z. Lanthanum/iron co-modified biochar for highly efficient adsorption of low-concentration phosphate from aqueous solution. J Environ Chem Eng. 2024;12(2):111876. doi: 10.1016/j.jece.2024.111876

79. Samoraj M, Mironiuk M, Witek-Krowiak A, Izydorczyk G, Skrzypczak D, Mikula K, et al. Biochar in environmental friendly fertilizers–Prospects of development products and technologies. Chemosphere. 2022;296:133975. doi: 10.1016/j.chemosphere.2022.133975
80. Wang C, Luo D, Zhang X, Huang R, Cao Y, Liu G, et al. Biochar-based slow-release of fertilizers for sustainable agriculture: A mini review. Environ Sci Ecotechnol. 2022;10:100167. doi: 10.1016/j.ese.2022.100167
81. Guo M, Song W, Tian J. Biochar-Facilitated Soil Remediation: Mechanisms and Efficacy Variations. Front Environ Sci. 2020;8:521512. doi: 10.3389/fenvs.2020.521512
82. Nguyen T, Ngo H, Guo W, Zhang J, Liang S, Lee D, et al. Modification of agricultural waste/by-products for enhanced phosphate removal and recovery: Potential and obstacles. Bioresour Technol. 2014;169:750-62. doi: 10.1016/j.biortech.2014.07.047
83. Haddad K, Jellali S, Jeguirim M, Trabelsi ABH, Limousy L. Investigations on phosphorus recovery from aqueous solutions by biochars derived from magnesium-pretreated cypress sawdust. J Environ Manag. 2018;216:305-14. doi: 10.1016/j.jenvman.2017.06.020
84. Genuino D, De Luna M, Capareda S. Improving the surface properties of municipal solid waste-derived pyrolysis biochar by chemical and thermal activation: Optimization of process parameters and environmental application. Waste Manag. 2018;72:255-64. doi: 10.1016/j.wasman.2017.11.038
85. Herath A, Layne C, Perez F, Hassan E, Pittman C, Mlsna T. KOH-activated high surface area Douglas fir biochar for adsorbing aqueous Cr(VI), Pb(II) and Cd(II). Chemosphere. 2021;269:128409. doi: 10.1016/j.chemosphere.2020.128409
86. Patra B, Nanda S, Dalai A, Meda V. Taguchi-based process optimization for activation of agro-food waste biochar and performance test for dye adsorption. Chemosphere. 2021;285:131531. doi: 10.1016/j.chemosphere.2021.131531
87. Gao AL, Wan Y. Iron modified biochar enables recovery and recycling of phosphorus from wastewater through column filters and flow reactors. Chemosphere. 2023;313:137434. doi: 10.1016/j.chemosphere.2022.137434
88. Ai D, Ma H, Meng Y, Wei T, Wang B. Phosphorus recovery and reuse in water bodies with simple ball-milled Ca-loaded biochar. Sci Total Environ. 2023;860:160502. doi: 10.1016/j.scitotenv.2022.160502
89. Qiu G, Zhao Y, Wang H, Tan X, Chen F, Hu X. Biochar synthesized via pyrolysis of Broussonetia papyrifera leaves: Mechanisms and potential applications for phosphate removal. Environ Sci Pollut Res. 2019;26:6565-75. doi: 10.1007/s11356-018-04095-w
90. Yin Q, Liu M, Ren H. Biochar produced from the co-pyrolysis of sewage sludge and walnut shell for ammonium and phosphate adsorption from water. J Environ Manag. 2019;249:109410. doi: 10.1016/j.jenvman.2019.109410

91. Mitrogiannis D, Psychoyou M, Baziotis I, Inglezakis VJ, Koukouzas N, Tsoukalas N, et al. Removal of phosphate from aqueous solutions by adsorption onto $Ca(OH)_2$ treated natural clinoptilolite. Chem Eng J. 2017;320:510-22. doi: 10.1016/j.cej.2017.03.063
92. Bashar R, Gungor K, Karthikeyan KG, Barak P. Cost effectiveness of phosphorus removal processes in municipal wastewater treatment. Chemosphere. 2018;197:280-90. doi: 10.1016/j.chemosphere.2017.12.169
93. Qiu H, Liang C, Yu J, Zhang Q, Song M, Chen F. Preferable phosphate sequestration by nano-La(III) (hydr)oxides modified wheat straw with excellent properties in regeneration. Chem Eng J. 2017;315:345-54. doi: 10.1016/j.cej.2017.01.043
94. Antunes E, Jacob MV, Brodie G, Schneider PA. Isotherms, kinetics and mechanism analysis of phosphorus recovery from aqueous solution by calcium-rich biochar produced from biosolids via microwave pyrolysis. J Environ Chem Eng. 2018;6:395-403. doi: 10.1016/j.jece.2017.12.011
95. Pap S, Gaffney PPJ, Bremner B, Turk Sekulic M, Maletic S, Gibb SW, et al. Enhanced phosphate removal and potential recovery from wastewater by thermo-chemically calcinated shell adsorbents. Sci Total Environ. 2022;814:152794. doi: 10.1016/j.scitotenv.2021.152794
96. Wang S, Kong L, Long J, Su M, Diao Z, Chang X, et al. Adsorption of phosphorus by calcium-flour biochar: Isotherm, kinetic and transformation studies. Chemosphere. 2018;195:666-72. doi: 10.1016/j.chemosphere.2017.12.101
97. Pérez S, Muñoz-Saldaña J, Garcia-Nunez JA, Acelas N, Flórez E. Unraveling the Ca–P species produced over the time during phosphorus removal from aqueous solution using biocomposite of eggshell–palm mesocarp fiber. Chemosphere. 2022;287:132333. doi: 10.1016/j.chemosphere.2021.132333
98. Köse TE, Kıvanç B. Adsorption of phosphate from aqueous solutions using calcined waste eggshell. Chem Eng J. 2011;178:34-9. doi: 10.1016/j.cej.2011.09.129
99. Naidu TS, Sheridan CM, van Dyk LZ. Basic oxygen furnace slag: Review of current and potential uses. Miner Eng. 2020;149:106234. doi: 10.1016/j.mineng.2020.106234
100. Li Y, Liu Y, Gong X, Nie Z, Cui S, Wang Z, Chen W. Environmental impact analysis of blast furnace slag applied to ordinary Portland cement production. J Clean Prod. 2016;120:221-30. doi: 10.1016/j.jclepro.2015.12.071
101. Barca C, Meyer D, Liira M, Drissen P, Comeau Y, Andrès Y, et al. Steel slag filters to upgrade phosphorus removal in small wastewater treatment plants: Removal mechanisms and performance. Ecol Eng. 2014;68:214-22. doi: 10.1016/j.ecoleng.2014.03.065
102. Johansson L, Gustafsson JP. Phosphate removal using blast furnace slags and opoka-mechanisms. Water Res. 2000;34(1):259-65. doi: 10.1016/S0043-1354(99)00135-9
103. Lee JY, Choi JS, Yuan TF, Yoon YS, Mitchell D. Comparing properties of concrete containing electric arc furnace slag and granulated blast furnace slag. Materials. 2019;12:1371. doi: 10.3390/ma12091371

104. Edgar M, Hamdan N, Morales D, Boyer TH. Phosphorus removal by steel slag from tile drainage water: Lab and field evaluations. Chemosphere. 2022;307:135850. doi: 10.1016/j.chemosphere.2022.135850
105. Westholm JL. The use of blast furnace slag for removal of phosphorus from wastewater in Sweden—A review. Water. 2010;2:826-37. doi: 10.3390/w2040826
106. Zhang S, Liu F, Zhu H, Lv S, Wang B. Simultaneous nitrate and phosphorus removal in novel steel slag biofilters: Optimization and mechanism study. J Environ Manag. 2024;349:119558. doi: 10.1016/j.jenvman.2023.119558
107. Wu F, Yu Q, Gauvin F, Brouwers HJH. A facile manufacture of highly adsorptive aggregates using steel slag and porous expanded silica for phosphorus removal. Resour Conserv Recycl. 2021;166:105238. doi: 10.1016/j.resconrec.2020.105238
108. Bobicki ER, Liu Q, Xu Z, Zeng H. Carbon capture and storage using alkaline industrial wastes. Prog Energy Combust. Sci. 2012;38(2):302-20. doi: 10.1016/j.pecs.2011.11.002
109. Bayer P, Heuer E, Karl U, Finkel M. Economical and ecological comparison of granular activated carbon (GAC) adsorber refill strategies. Water Res. 2005;39(9):1719-28. doi: 10.1016/j.watres.2005.02.005
110. Kaasik A, Vohla C, Mõtlep R, Mander Ü, Kirsimäe K. Hydrated calcareous oil-shale ash as potential filter rmedia for phosphorus removal in constructed wetlands. Water Res. 2008;42:1315-23. doi: 10.1016/j.watres.2007.10.002
111. Kõiv M, Liira M, Mander Ü., Mõtlep R, Vohla C, Kirsimäe K. Phosphorus removal using Ca-rich hydrated oil shale ash as filter material—The effect of different phosphorus loadings and wastewater compositions. Water Res. 2010;44:5232-39. doi: 10.1016/j.watres.2010.06.044
112. Kasak K, Mõtlep R, Truu M, Truu J, Kõiv-Vainik M, Espenberg M, et al. Hydrated oil shale ash mitigates greenhouse gas emissions from horizontal subsurface flow filters for wastewater treatment. Water Air Soil Pollut. 2016;227:320. doi: 10.1007/s11270-016-3007-8
113. Zhou H, Bhattarai R, Li Y, Li S, Fan Y. Utilization of coal fly and bottom ash pellet for phosphorus adsorption: Sustainable management and evaluation. Resour Conserv Recycl. 2019;149:372-80. doi: 10.1016/j.resconrec.2019.06.017
114. Xu R, Lyu T, Wang L, Yuan Y, Zhang M, Cooper M, et al. Utilization of coal fly ash waste for effective recapture of phosphorus from waters. Chemosphere. 2022;287:132431. doi: 10.1016/j.chemosphere.2021.132431
115. Li S, Cooke RA, Wang L, Ma F, Bhattarai R. Characterization of fly ash ceramic pellet for phosphorus removal. J Environ Manag. 2017;189:67-74. doi: 10.1016/j.jenvman.2016.12.042
116. Li S, Cooke RA, Huang X, Christianson L, Bhattarai R. Evaluation of fly ash pellets for phosphorus removal in a laboratory scale denitrifying bioreactor. J Environ Manag. 2018;207:269-75. doi: 10.1016/j.jenvman.2017.11.040
117. Jeong I, Kim K. Utilizing a granulated coal bottom ash and oyster shells for nutrient removal in eutrophic sediments. Mar Pollut Bull. 2022;177:113549. doi: 10.1016/j.marpolbul.2022.113549

118. Singh NB, Agarwal A, De A, Singh P. Coal fly ash: An emerging material for water remediation. Int J Coal Sci Technol. 2022;9(1):44. doi: 10.1007/s40789-022-00512-1
119. Asaoka S, Kawakami K, Saito H, Ichinari T, Nohara H, Oikawa T. Adsorption of phosphate onto lanthanum-doped coal fly ash—Blast furnace cement composite. J Hazard Mater. 2021;406:124780. doi: 10.1016/j.jhazmat.2020.124780
120. Somna K, Jaturapitakkul C, Kajitvichyanukul P, Chindaprasirt P. NaOH-activated ground fly ash geopolymer cured at ambient temperature. Fuel. 2011;90(6):2118-24. doi: 10.1016/j.fuel.2011.01.018
121. Mucci M, Maliaka V, Noyma N, Marinho M, Lürling M. Assessment of possible solid-phase phosphate sorbents to mitigate eutrophication: Influence of pH and anoxia. Sci Total Environ. 2018;619-620:1431-40. doi: 10.1016/j.scitotenv.2017.11.198
122. Cusack PB, Healy MG, Ryan PC, Burke IT, O'Donoghue LMT, Ujaczki É, et al. Enhancement of bauxite residue as a low-cost adsorbent for phosphorus in aqueous solution, using seawater and gypsum treatments. J Clean Prod. 2018;179:217-24. doi: 10.1016/j.jclepro.2018.01.092
123. Newson T, Dyer T, Adam C, Sharp S. Effect of structure on the geotechnical properties of bauxite residue. J Geotech Geoenviron Eng. 2006;132(2):143-51. doi: 10.1061/(ASCE)1090-0241(2006)132:2(143)
124. Barca C, Magari M, Miche M, Hennebert H. Effect of different wastewater composition on kinetics, capacities, and mechanisms of phosphorus sorption by carbonated bauxite residue. J Environ Chem Eng. 2022;10:108922. doi: 10.1016/j.jece.2022.108922
125. Li Y, Haynes RJ, Chandrawana I, Zhou YF. Growth of Rhodes grass and leaching of ions from seawater neutralized bauxite residues after amendment with gypsum and organic wastes. J Environ Manag. 2019;231:596-604. doi: 10.1016/j.jenvman.2018.10.083
126. Liu Y, Lin C, Wu Y. Characterization of red mud derived from a combined Bayer process and bauxite calcination method. J Hazard Mater. 2007;146:255-61. doi: 10.1016/j.jhazmat.2006.12.015
127. Park JH, Wang JJ, Seo DC. Sorption characteristics of phosphate by bauxite residue in aqueous solution. Colloids Surf A Physicochem Eng Asp. 2021;618:126465. doi: 10.1016/j.colsurfa.2021.126465
128. Yang J, Ma X, Xiong Q, Zhou X, Wu H, Yan S, et al. Functional biochar fabricated from red mud and walnut shell for phosphorus wastewater treatment: Role of minerals. Environ Res. 2023;232:116348. doi: 10.1016/j.envres.2023.116348
129. Sima TV, Letshwenyo MW, Lebogang L. Efficiency of waste clinker ash and iron oxide tailings for phosphorus removal from tertiary wastewater: Batch studies. Environ Technol Innov. 2018;11:49-63. doi: 10.1016/j.eti.2018.04.008
130. Christianson LE, Lepine C, Sibrell PL, Penn C, Summerfelt ST. Denitrifying woodchip bioreactor and phosphorus filter pairing to minimize pollution swapping. Water Res. 2017;121:129-39. doi: 10.1016/j.watres.2017.05.026

131. Dobbie KE, Heal KV, Aumônier J, Smith KA, Johnston A, Younger PL. Evaluation of iron ochre from mine drainage treatment for removal of phosphorus from wastewater. Chemosphere. 2009;75(6):795-800. doi: 10.1016/j.chemosphere.2008.12.049
132. Al-Mallahi J, Sürmeli RÖ, Çalli B. Recovery of phosphorus from liquid digestate using waste magnesite dust. J Clean Prod. 2020;272:122616. doi: 10.1016/j.jclepro.2020.122616
133. Nättorp A, Remmen K, Remy C. Cost assessment of different routes for phosphorus recovery from wastewater using data from pilot and production plants. Water Sci Technol. 2017;76(2):413-24. doi: 10.2166/wst.2017.212
134. Duranceau SJ, Biscardi PG. Comparing adsorptive media use for the direct treatment of phosphorous-impaired surface water. J Environ Eng. 2015;141(8):04015012. doi: 10.1061/(ASCE)EE.1943-7870.0000951
135. Babatunde AO, Zhao YQ. Equilibrium and kinetic analysis of phosphorus adsorption from aqueous solution using waste alum sludge. J Hazard Mater. 2010;184(1-3):746-52. doi: 10.1016/j.jhazmat.2010.08.102
136. Ayoub G, Kalinin H. Removal of low-concentration phosphorus using a fluidized raw dolomite bed. Water Environ Res. 2006;78(4):353-61. doi: 10.2175/106143005X90001
137. Wang X, Chen J, Kong Y, Shi X. Sequestration of phosphorus from wastewater by cement-based or alternative cementitious materials. Water Res. 2014;62:88-96. doi: 10.1016/j.watres.2014.05.021
138. Egemose S, Sønderup MJ, Beinthin MV, Reitzel K, Hoffmann CC, Flindt MR. Crushed concrete as a phosphate binding material: A potential new management tool. J Environ Qual. 2012;41(3):647-53. doi: 10.2134/jeq2011.0134

How to cite this article:
Ozola-Davidane R, Gruskevica K, Purmalis O, Kostjukova S, Karasa J, Zekker, I, et al. Sustainable sorbent materials for phosphorus removal and recovery from wastewater: a comprehensive review and TRL-based evaluation. J Sustain Res. 2026;8(2):e260043. https://doi.org/10.20900/jsr20260043.